Experimental Physiology – *Research Paper*

Dynamic characteristics of heart rate control by the autonomic nervous system in rats

Masaki Mizuno[1,2], Toru Kawada[2], Atsunori Kamiya[2], Tadayoshi Miyamoto[2,3], Shuji Shimizu[2], Toshiaki Shishido[2], Scott A. Smith[1] and Masaru Sugimachi[2]

[1]*Departments of Physical Therapy and Internal Medicine, University of Texas Southwestern Medical Center at Dallas, TX, USA*
[2]*Department of Cardiovascular Dynamics, National Cerebral and Cardiovascular Center Research Institute, Osaka, Japan*
[3]*Department of Physical Therapy, Morinomiya University of Medical Sciences, Osaka, Japan*

We estimated the transfer function of autonomic heart rate (HR) control by using random binary sympathetic or vagal nerve stimulation in anaesthetized rats. The transfer function from sympathetic stimulation to HR response approximated a second-order, low-pass filter with a lag time (gain, 4.29 ± 1.55 beats min^{-1} Hz^{-1}; natural frequency, 0.07 ± 0.03 Hz; damping coefficient, 1.96 ± 0.64; and lag time, 0.73 ± 0.12 s). The transfer function from vagal stimulation to HR response approximated a first-order, low-pass filter with a lag time (gain, 8.84 ± 4.51 beats min^{-1} Hz^{-1}; corner frequency, 0.12 ± 0.06 Hz; and lag time, 0.12 ± 0.08 s). These results suggest that the dynamic characteristics of HR control by the autonomic nervous system in rats are similar to those of larger mammals.

(Received 5 March 2010; accepted after revision 24 May 2010; first published online 28 May 2010)
Corresponding author M. Mizuno: Department of Physical Therapy, University of Texas Southwestern Medical Center at Dallas, 5323 Harry Hines Boulevard, Dallas, TX 75390-9174, USA. Email: masaki.mizuno@utsouthwestern.edu

Despite extensive use of rats in cardiovascular research, the dynamic characteristics of heart rate (HR) control by the autonomic nervous system in this species remain to be elucidated. To better understand the autonomic control of HR in rats, it is important to quantitatively assess the input–output relationship between autonomic nerve stimulation and HR over a wide range of frequencies that are of physiological interest. By understanding these relationships in the rat, data obtained using this animal model may be more readily extrapolated to larger mammals, including humans.

Heart rate variability is considered to reflect autonomic tone because its components change both physiologically (e.g. standing and ageing) and pathophysiologically (e.g. hypertension and heart failure; Malliani *et al.* 1991). Based on dog and human studies, the very low-frequency (VLF) component (0.02–0.08 Hz) is likely to reflect changes in vasomotor tone in relation to thermoregulation and local adjustment of resistance in individual vascular beds; the low-frequency (LF) component (0.08–0.15 Hz) is considered to be Mayer's wave and a marker of sympathetic activity; and the high-frequency (HF) component (0.15–0.40 Hz) mainly originates from respiratory activity and is considered to be mediated by vagal activity (Pagani *et al.* 1986). Based on the differences in HR spectra between conscious rats and rats in which autonomic blockade was induced pharmacologically, Cerutti *et al.* (1991) determined that the VLF component ranged between 0.017 and 0.26 Hz, the LF component ranged between 0.27 and 0.74 Hz, and the HF component was above 0.75 Hz. Even though these allocations in frequency band in rats corresponded to their considerably higher basal HR (range between 300 and 400 beats min^{-1}) compared with that of larger mammals, such as dogs and humans (range between 60 and 100 beats min^{-1}), there has been no scientific rationale provided for setting these allocations. This is because it is unknown whether the dynamic characteristics of HR control by the autonomic nervous system in rats are significantly different from those in larger mammals, such as rabbits (Kawada *et al.* 1996), cats (Chess & Calaresu, 1971) and dogs (Berger *et al.* 1989).

Given that the release and disposition of neurotransmitters (e.g. noradrenaline and acetylcholine) at autonomic nerve endings may be determined biochemically, regardless of body size, we hypothesized that the dynamic characteristics of HR control by the autonomic nervous system would not differ appreciably among different mammalian species. To test this

DOI: 10.1113/expphysiol.2010.053090

hypothesis, we quantified the dynamic characteristics of HR control mediated by sympathetic or vagal nerve stimulation in rats using transfer function analysis. The results provide the first quantitative data on the dynamic characteristics of autonomic HR regulation in rats. Since HR changes dynamically in response to daily activities, quantification of how quickly the HR can respond to sympathetic or vagal nerve stimulation is important. For instance, information on the dynamic HR response is key to understanding the generation of HR variability. The present study aims to expand our knowledge of HR control by the autonomic nervous system.

Methods

Surgical preparation

Animal care was in accordance with the *Guiding Principles for Care and Use of Animals in the Field of Physiological Sciences*, approved by the Physiological Society of Japan. All protocols were reviewed and approved by the Animal Subjects Committee of the National Cerebral and Cardiovascular Center. Thirteen Sprague–Dawley rats (body weight, 340–670 g) were anaesthetized using a mixture of urethane (250 mg ml^{-1}; Sigma, St. Louis, MO, USA) and α-chloralose (40 mg ml^{-1}; Sigma), initiated with an intraperitoneal bolus injection of 1 ml kg^{-1}. If additional anaesthesia was needed, 0.1 ml kg^{-1} was given intraperitoneally. The rats were intubated and mechanically ventilated with oxygen-enriched room air. The rats were slightly hyperventilated to suppress chemoreflexes (arterial P_{CO_2} ranged from 30 to 35 mmHg; arterial P_{O_2} > 300 mmHg). Arterial blood pH was within the physiological range. A catheter was placed in the right femoral artery, which was connected to a pressure transducer (DX-200, Nihon Kohden, Tokyo, Japan) to measure arterial pressure (AP). Heart rate was measured using a cardiotachometer (AT601G, Nihon Kohden, Tokyo, Japan) triggered by the R wave on the electrocardiogram. The HR series were checked by visual inspection. A catheter was introduced into the right femoral vein for drug administration. Sino-aortic denervation was performed bilaterally to minimize changes in the sympathetic efferent nerve activity via arterial baroreflexes. The vagi were sectioned bilaterally at the neck. A pair of bipolar stainless-steel electrodes was attached to the right cervical sympathetic nerve for efferent sympathetic stimulation or the right cervical vagus for efferent vagal stimulation. The stimulation electrodes and nerve were secured with silicon glue (Kwik-Sil, World Precision Instruments, Sarasota, FL, USA). Body temperature was monitored with a thermometer placed in the rectum, and was maintained at 38°C with a heating pad throughout the experiment.

Experimental procedures

The pulse duration was set at 2 ms and the stimulation amplitude was fixed at 10 V for both sympathetic and vagal nerve stimulation. To allow stable haemodynamics, sympathetic and vagal nerve stimulation was started at ~1 h after the end of surgical preparation. Between sympathetic and vagal stimulation protocols, >15 min elapsed to allow AP and HR to return to their respective baseline values.

To estimate the dynamic transfer characteristics from sympathetic stimulation to the HR response, the sectioned end of the right cervical sympathetic nerve was stimulated, employing a frequency-modulated pulse train for 10 min. The stimulation frequency was switched every 1000 ms to either 0 or 5 Hz, according to a binary white-noise signal. The power spectrum of the stimulation signal was reasonably constant up to 0.5 Hz. The transfer function was estimated up to 0.5 Hz because the reliability of estimation decreased owing to the diminution of input power above this frequency. The selected frequency range was determined based on previous results in rabbits (Kawada *et al.* 1996) so that it would sufficiently span the physiological range of interest with respect to the dynamic sympathetic control of HR.

To estimate the dynamic transfer characteristics from vagal stimulation to the HR response, the right vagus was stimulated, employing a frequency-modulated pulse train for 10 min. The stimulation frequency was switched every 500 ms to either 0 or 10 Hz, according to a binary white-noise signal. The power spectrum of the stimulation signal was reasonably constant up to 1 Hz. The transfer function was estimated up to 1 Hz because the reliability of estimation decreased owing to the diminution of input power above this frequency. The selected frequency range was determined based on previous results in rabbits (Kawada *et al.* 1996) so that it would sufficiently span the physiological range of interest with respect to the dynamic vagal control of HR.

The switching intervals differed between sympathetic and vagal stimulation for the following reasons. In theory, the switching interval of binary white noise is inversely related to an upper frequency bound for the input modulation frequency. Prior knowledge in rabbits (Kawada *et al.* 1996) and preliminary results in rats indicated that the upper frequency bound of physiological interest might be lower for the sympathetic transfer function, which rendered the switching interval longer for the sympathetic stimulation. Another reason relates to the stimulation frequency. In the present study, the sympathetic stimulation frequency of 5 Hz and the vagal stimulation frequency of 10 Hz were determined based on the HR response. Once the stimulation frequency is determined, there is a methodological limitation for setting the switching interval. For example, a switching

interval of 500 ms is too close to a pulse interval of 200 ms (i.e. 5 Hz stimulation). In this case, only two pulses can be applied in the shortest interval of 500 ms, which means that the stimulation frequency may be in effect 4 Hz rather than the intended 5 Hz. This problem does not occur with a 1000 ms switching interval in combination with 5 Hz stimulation and 500 ms switching interval in combination with 10 Hz stimulation.

Background sympathetic tone is known to augment vagal HR control (an accentuated antagonism; Levy, 1971; Kawada *et al.* 1996). To eliminate any effect of sympathetic activity, in seven out of the thirteen rats the vagal stimulation protocol was repeated after the administration of the β-adrenergic blocker propranolol (1 mg kg^{-1} I.V.; Perlini *et al.* 1995).

Data analysis

Data were digitized at 200 Hz using a 12 bit analog-to-digital converter and stored on the hard disk of a dedicated laboratory computer system. The dynamic transfer function from binary white-noise stimulation to the HR response was estimated based on the following procedure. To avoid the possibility that the initial transition from no stimulation to random stimulation biased the transfer function estimation, data were processed only from 2 min after the initiation of random stimulation. Input–output data pairs of the stimulation frequency and HR were resampled at 10 Hz. Subsequently, data pairs were partitioned into eight 50%-overlapping segments consisting of 1024 data points each. For each segment, the linear trend was subtracted and a Hanning window was applied. A fast Fourier transform was then performed to obtain the frequency spectra of nerve stimulation [$N(f)$] and HR [$HR(f)$]. Over the eight segments, the power of the nerve stimulation [$S_{N\cdot N}(f)$], the power of the HR [$S_{HR\cdot HR}(f)$], and the cross-power between these two signals [$S_{N\cdot HR}(f)$] were ensemble averaged. Finally, the transfer function [$\mathrm{H}(f)$] from nerve stimulation to the HR response was determined using the following equation (Marmarelis & Marmarelis, 1978):

$$\mathrm{H}(f) = \frac{S_{N\cdot HR}(f)}{S_{N\cdot N}(f)} \tag{1}$$

To quantify the linear dependence of the HR response on vagal or sympathetic stimulation, the magnitude-squared coherence function [$\mathrm{Coh}(f)$] was estimated by employing the following equation (Marmarelis & Marmarelis, 1978):

$$\mathrm{Coh}(f) = \frac{|S_{N\cdot HR}(f)|^2}{S_{N\cdot N}(f) \times S_{HR\cdot HR}(f)} \tag{2}$$

Coherence values range from zero to unity. Unity coherence indicates perfect linear dependence between the input and output signals; in contrast, zero coherence indicates total independence between the two signals.

As preliminary results suggested that the transfer function from sympathetic stimulation to HR response in rats approximated a second-order low-pass filter with pure delay, as in the case of rabbits (Kawada *et al.* 1996, 2009), we determined the parameters of the sympathetic transfer function using the following equation:

$$\mathrm{H}(f) = \frac{K}{1 + 2\zeta\frac{f}{f_\mathrm{N}}j + \left(\frac{f}{f_\mathrm{N}}j\right)^2} \mathrm{e}^{-2\pi f j L} \tag{3}$$

where K is dynamic gain (in beats per minute per herz), f_N is the natural frequency (in herz), ζ is the damping ratio, L is lag time (in seconds), and f and j represent frequency and imaginary units, respectively. The dynamic gain (K, in beats per minute per herz) represents the asymptotic value of transfer gain as the frequency approaches zero, and corresponds to the steady-state response in the step response. The natural frequency (f_N, in herz) determines the frequency limit of the low-pass filter above which the transfer gain reduces as the frequency increases. In the second-order low-pass filter, the maximal negative slope of the gain diminution is 1/100 per 10 Hz. The damping ratio (ζ, unitless) characterizes how the transfer gain varies around the f_N. The lag time (L, in seconds) indicates the latency of signal transmission from nerve stimulation to the initiation of HR response. These parameters were estimated by means of an iterative non-linear least-squares regression.

As preliminary results suggested that the transfer function from vagal stimulation to HR response in rats approximated a first-order low-pass filter with pure delay, as in the case of rabbits (Kawada *et al.* 1996, 2009), we determined the parameters of the vagal transfer function using the following equation:

$$\mathrm{H}(f) = \frac{-K}{1 + \frac{f}{f\mathrm{c}}j} \mathrm{e}^{-2\pi f j L} \tag{4}$$

where K represents the dynamic gain (in beats per minute per herz), $f\mathrm{c}$ denotes the corner frequency (in herz), L denotes the lag time (in seconds), and f and j represent frequency and imaginary units, respectively. The negative sign in the numerator indicates the negative HR response to vagal stimulation. The dynamic gain (K, in beats per minute per herz) represents the asymptotic value of transfer gain as the frequency approaches zero. The corner frequency ($f\mathrm{c}$, in herz) represents the frequency at which the transfer gain decreases by 3 dB relative to K. Higher $f\mathrm{c}$ indicates the more rapid HR response to vagal stimulation. In the first-order low-pass filter, the maximal slope of the gain diminution is 1/10 per 10 Hz. The lag time (L, in seconds) indicates the latency of signal transmission from nerve stimulation to the initiation of HR response. These

parameters were estimated by means of an iterative non-linear least-squares regression.

To facilitate the intuitive understanding of the system's dynamic characteristics, we calculated the system step response of HR to 1 Hz nerve stimulation as follows. The system impulse response was derived from the inverse Fourier transform of $H(f)$. The system step response was then obtained from the time integral of the impulse response. The length of the step response was 51.2 s. The 80% rise time for sympathetic step response or the 80% fall time for vagal step response was estimated at the time which the step response reached 80% of the steady-state response, calculated by averaging the last 10 s of data from the step response.

Statistical analysis

All data are represented as means ± S.D. Student's paired *t* test was used to test differences in haemodynamic parameters. In seven rats, parameters of vagal transfer function were compared before and after propranolol administration using Student's paired *t* test. Values of $P < 0.05$ were considered significant.

Results

Typical recordings

Figure 1 shows typical recordings of sympathetic and vagal stimulation obtained from one rat. While HR varied immediately during random vagal stimulation, it changed only gradually during random sympathetic stimulation. Sympathetic stimulation increased the mean HR from 375.5 ± 33.5 to 444.9 ± 28.4 beats min^{-1} ($P < 0.05$); vagal stimulation decreased the mean HR from 378.2 ± 31.9 to 317.3 ± 47.1 beats min^{-1} ($P < 0.05$). Neither sympathetic nor vagal stimulation altered mean AP (79.1 ± 18.4 *versus* 75.1 ± 19.4 and 78.2 ± 20.2 *versus* 72.4 ± 18.3 mmHg, respectively).

Sympathetic transfer function

Figure 2*A* illustrates the dynamic transfer function characterizing sympathetic HR control averaged from all animals. Gain plots, phase plots and coherence functions are shown. The sympathetic transfer function approximated a second-order, low-pass filter with a lag time (dynamic gain, 4.29 ± 1.55 beats min^{-1} Hz^{-1}; natural frequency, 0.07 ± 0.03 Hz; damping coefficient, 1.96 ± 0.64; and lag time, 0.73 ± 0.12 s). Figure 2*B* shows the calculated step response of HR to sympathetic stimulation averaged from all animals. As expected, sympathetic stimulation gradually increased HR. The steady-state sympathetic response was 3.86 ± 1.80 beats min^{-1} Hz^{-1}. The 80% rise time for the sympathetic step response was 13.7 ± 5.1 s.

Vagal transfer function

Figure 2*C* illustrates the dynamic transfer function characterizing vagal HR control averaged from all animals. The vagal transfer function approximated a first-order, low-pass filter with a lag time (dynamic gain, 8.84 ± 4.51 beats min^{-1} Hz^{-1}; corner frequency, 0.12 ± 0.06 Hz; and lag time, 0.12 ± 0.08 s). Figure 2*D* shows the calculated step response of HR to vagal

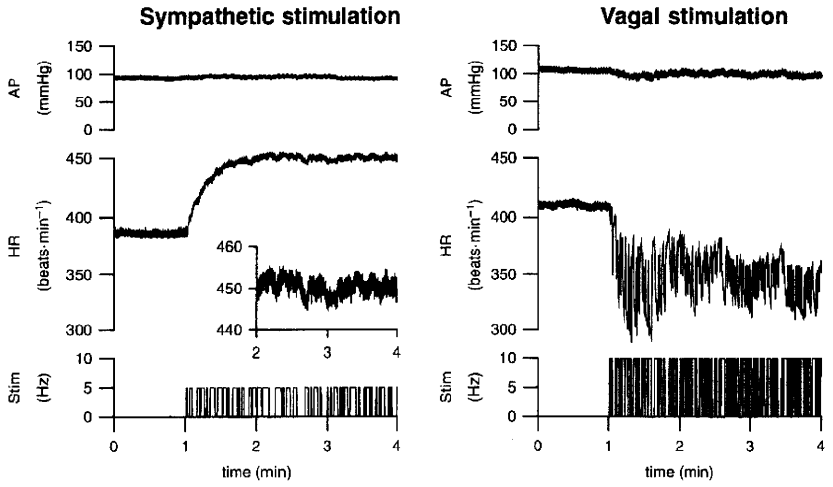

Figure 1. Raw trace of 10 Hz resampled arterial pressure (AP; top) and heart rate (HR; middle) obtained using binary white-noise stimulation (Stim; bottom)
Recordings are shown for sympathetic (left) and vagal nerve stimulation (right). The inset in the panels for sympathetic stimulation indicates the expanded ordinate for the HR response.

stimulation averaged from all animals. As expected, vagal stimulation decreased HR. The vagal HR response appeared more quickly than the sympathetic HR response. The steady-state vagal response was 9.63 ± 5.21 beats min^{-1} Hz^{-1}. The 80% fall time for the vagal step response was 4.13 ± 1.74 s.

β-Adrenergic blockade did not significantly affect any parameters of the vagal transfer function (dynamic gain, 7.96 ± 2.97 *versus* 7.75 ± 2.49 beats min^{-1} Hz^{-1}; corner frequency, 0.12 ± 0.05 *versus* 0.11 ± 0.05 Hz; and lag time, 0.10 ± 0.08 *versus* 0.17 ± 0.08 s, before and after β-adrenergic blockade, respectively).

Discussion

We have demonstrated the first quantitative data on the dynamic characteristics of HR control by the sympathetic and vagal nerves in rats. These results suggest that the dynamic characteristics of autonomic HR control in rats are similar to those of larger mammals despite basal HR being higher in these animals.

Sympathetic transfer function

In the present study, we stimulated the preganglionic cardiac sympathetic nerve instead of the postganglionic cardiac sympathetic nerve because of technical reasons. Therefore, the sympathetic transfer function was estimated from the combined dynamic characteristics of ganglionic and postganglionic transmission. Nevertheless, the sympathetic transfer function approximated a second-order delay system (Fig. 2*A*) and its parameters were similar to those estimated between postganglionic sympathetic stimulation and HR response in rabbits

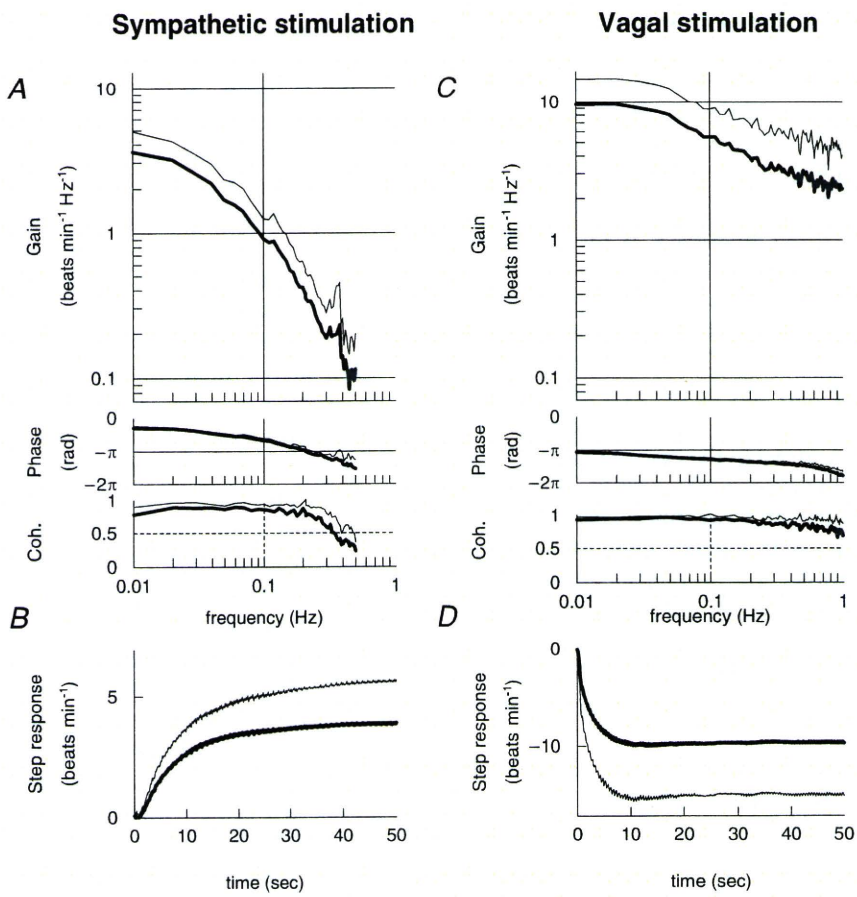

Figure 2. Transfer functions and step responses of HR to sympathetic and vagal stimulation
A, dynamic transfer function relating sympathetic stimulation to the HR response averaged from all animals. Gains (top), phase shifts (middle) and coherence functions (bottom) are presented. *B*, calculated step response to 1 Hz tonic sympathetic stimulation averaged from all animals. *C*, dynamic transfer function relating vagal stimulation to the HR response averaged from all animals. Gains (top), phase shifts (middle) and coherence functions (bottom) are presented. *D*, calculated step response to 1 Hz tonic vagal stimulation averaged from all animals. Thick lines represent the mean, whereas thin lines indicate + S.D. values.

(natural frequency, 0.06–0.07 Hz; damping coefficient, 1.34–1.53; and lag time, 0.51–0.65 s; Kawada *et al.* 2009). If we calculate the corner frequency (frequency at which gain decreased by 3 dB from steady-state gain; 0.04 ± 0.01 Hz) instead of natural frequency, our results are comparable to the corner frequency (0.01–0.02 Hz) found by Berger *et al.* (1989) using dogs. Thus, in the present study sympathetic transfer function in rats resembles that of dogs. The 80% rise time for sympathetic step response is also comparable to that of rabbits (14.4–17.2 s) as reported by Kawada *et al.* (2009). Therefore, we contend that the dynamic characteristics in ganglionic transmission contribute little to the determination of the overall low-pass characteristics of sympathetic HR control.

Vagal transfer function

The transfer function of vagal stimulation to HR response can be characterized as a first-order delay system (Fig. 2*C*), as in previous reports using rabbits (Kawada *et al.* 1996), dogs (Berger *et al.* 1989) and cats (Chess & Calaresu, 1971). The estimated corner frequency of the transfer function from vagal stimulation to HR response in the present study (0.12 ± 0.06 Hz) is different but of the same order as that of rabbits (0.39 Hz; Kawada *et al.* 2009) and cats (0.05 Hz; Chess & Calaresu, 1971). However, if we calculate the corner frequency as the frequency at which gain decreases by 3 dB from steady-state gain, the value is 0.06 ± 0.01 Hz. Furthermore, the 80% fall time for the vagal step response in rats is also greater than that in rabbits (1.3 s; Kawada *et al.* 2009). Hence, the first-order low-pass filter may not be the best approximation of the transfer function from vagal stimulation to HR response in rats, in contrast to the case in rabbits (Kawada *et al.* 1996, 2009) Furthermore, Berger *et al.* (1989) demonstrated that the effective filter characteristics of the system depend on the mean level of stimulatory rates. Additional studies are needed to clarify some of the disparity in results between the present investigation and other reports. Overall, however, the dynamic transfer function characteristics of HR regulation by the vagus were not appreciably different in rats compared with larger mammals.

Although sino-aortic denervation should have minimized the baroreflex-mediated changes in sympathetic nerve activity, this procedure does not necessarily eliminate the background sympathetic tone. It should be noted that tonic sympathetic stimulation may increase the dynamic gain of the vagal transfer function via accentuated antagonism (Kawada *et al.* 1996). The results of propranolol administration indicated that the effects of background sympathetic tone on the dynamic vagal control of HR were insignificant in the present study.

Physiological implications and perspectives

As mentioned in the Introduction, the allocations in frequency band of HR variability in rats (Cerutti *et al.* 1991) are set in a higher frequency band compared with those of larger mammals, such as dogs and humans (Malliani *et al.* 1991). However, parameters of dynamic characteristics in HR control by the autonomic nervous system in rats were not much different from those reported in larger mammals, suggesting the importance of biochemical processes of neurotransmitter release and disposition in determining dynamic HR response. Therefore, the allocations of HR variability in the HF component in rats may not readily be explained in terms of the dynamic characteristics of HR response to sympathetic and vagal nerve stimulation. Nevertheless, the fact that the vagal HR control is much faster than the sympathetic HR control may contribute to the generation of frequency dependence of HR variability.

To simply identify the dynamic characteristics of HR control by the autonomic nervous system in rats, the present study used Sprague–Dawley rats as normal animals. It has been well documented that exercise training results in increased vagal tone (Coote, 2010) and that pathophysiological conditions, such as chronic heart failure and hypertension, result in increased basal sympathetic tone (Billman, 2009) compared with the normal conditions. Further investigations are needed to clarify the impacts of such physiological and pathophysiological conditions on dynamic characteristics of HR control by the autonomic nervous system in rats.

The absolute gain values of the vagal transfer function seem higher than those previously reported in rabbits (Kawada *et al.* 1996, 2009). In those previous studies, the amplitude of vagal stimulation was adjusted in each animal so that HR was decreased by approximately 50 beats min^{-1} with 5 Hz tonic vagal stimulation. As a result, the stimulation amplitude was below 10 V. In the present study, however, the stimulation amplitude was fixed at 10 V, which would partly account for the larger gain values in the vagal transfer function. The absolute gain values are also affected by the operating HR. When the operating HR is within the saturation range of the HR response, the absolute gain values should be attenuated (Kawada *et al.* 1996). In addition, the magnitude of transfer gain is dependent on a mean stimulation frequency (Berger *et al.* 1989). Accordingly, direct comparison of the absolute gain values among different studies may be difficult based on the currently available data alone.

Limitations

There are several limitations to this study. First, data were obtained from anaesthetized animals. Since anaesthesia affects autonomic tone, the results may not be directly

applicable to conscious animals. Second, we stimulated the autonomic nerve according to binary white noise, which was quite different from the pattern of physiological neuronal discharge. However, the fact that coherence was near unity over the frequency range of interest indicates that, by virtue of their inherent linearity, the system properties would not vary much with differing patterns of stimulation. Finally, we measured AP using a femoral catheter connected to a fluid-filled pressure transducer. Although the computation of the mean pressure might be adequate, a reliable measurement of systolic/diastolic pressure would be difficult in the present study.

Conclusion

In the present study, it was demonstrated for the first time in rats that the transfer function from sympathetic stimulation to HR response approximated a second-order, low-pass filter with a lag time and that from vagal stimulation to HR response approximated a first-order, low-pass filter with a lag time. Despite the large difference in baseline HR, parameters of dynamic characteristics in HR control by the autonomic nervous system in rats are not much different from those reported in larger mammals. As such, the rat can be used as a reliable model for the determination of these parameters.

References

Berger RD, Saul JP & Cohen RJ (1989). Transfer function analysis of autonomic regulation. I. Canine atrial rate response. *Am J Physiol Heart Circ Physiol* **256**, H142–H152.

Billman GE (2009). Cardiac autonomic neural remodeling and susceptibility to sudden cardiac death: effect of endurance exercise training. *Am J Physiol Heart Circ Physiol* **297**, H1171–H1193.

Cerutti C, Gustin MP, Paultre CZ, Lo M, Julien C, Vincent M & Sassard J (1991). Autonomic nervous system and cardiovascular variability in rats: a spectral analysis approach. *Am J Physiol Heart Circ Physiol* **261**, H1292–H1299.

Chess GF & Calaresu FR (1971). Frequency response model of vagal control of heart rate in the cat. *Am J Physiol* **220**, 554–557.

Coote JH (2010). Recovery of heart rate following intense dynamic exercise. *Exp Physiol* **95**, 431–440.

Kawada T, Ikeda Y, Sugimachi M, Shishido T, Kawaguchi O, Yamazaki T, Alexander J Jr & Sunagawa K (1996). Bidirectional augmentation of heart rate regulation by autonomic nervous system in rabbits. *Am J Physiol Heart Circ Physiol* **271**, H288–H295.

Kawada T, Mizuno M, Shimizu S, Uemura K, Kamiya A & Sugimachi M (2009). Angiotensin II disproportionally attenuates dynamic vagal and sympathetic heart rate controls. *Am J Physiol Heart Circ Physiol* **296**, H1666–H1674.

Levy MN (1971). Sympathetic-parasympathetic interactions in the heart. *Circ Res* **29**, 437–445.

Malliani A, Pagani M, Lombardi F & Cerutti S (1991). Cardiovascular neural regulation explored in the frequency domain. *Circulation* **84**, 482–492.

Marmarelis P & Marmarelis V (1978). The white noise method in system identification. In *Analysis of Physiological Systems*, pp. 131–221. Plenum, New York.

Pagani M, Lombardi F, Guzzetti S, Rimoldi O, Furlan R, Pizzinelli P, Sandrone G, Malfatto G, Dell'Orto S, Piccaluga E, Turiel M, Baselli G, Cerutti S & Malliani A (1986). Power spectral analysis of heart rate and arterial pressure variabilities as a marker of sympatho-vagal interaction in man and conscious dog. *Circ Res* **59**, 178–193.

Perlini S, Giangregorio F, Coco M, Radaelli A, Solda PL, Bernardi L & Ferrari AU (1995). Autonomic and ventilatory components of heart rate and blood pressure variability in freely behaving rats. *Am J Physiol Heart Circ Physiol* **269**, H1729–H1734.

Acknowledgements

This study was supported by Health and Labor Sciences Research Grants (H18-nano-Ippan-003, H19-nano-Ippan-009, H20-katsudo-Shitei-007 and H21-nano-Ippan-005) from the Ministry of Health, Labor and Welfare of Japan, by Grants-in-Aid for Scientific Research (no. 19700559) from the Ministry of Education, Culture, Sports, Science and Technology in Japan and by the Industrial Technology Research Grant Program from New Energy and Industrial Technology Development Organization (NEDO) of Japan. M. Mizuno was supported by Research Fellowships of the Japan Society for the Promotion of Science for Young Scientists.

Autonomic Neuroscience: Basic and Clinical 156 (2010) 149–151

Contents lists available at ScienceDirect

Autonomic Neuroscience: Basic and Clinical

journal homepage: www.elsevier.com/locate/autneu

Short communication

Large conductance Ca^{2+}-activated K^+ channels inhibit vagal acetylcholine release at the rabbit sinoatrial node

Toru Kawada [a,*], Tsuyoshi Akiyama [b], Shuji Shimizu [a], Atsunori Kamiya [a], Kazunori Uemura [a], Yusuke Sata [a], Mikiyasu Shirai [b], Masaru Sugimachi [a]

[a] Department of Cardiovascular Dynamics, National Cerebral and Cardiovascular Center Research Institute, Osaka, Japan
[b] Department of Cardiac Physiology, National Cerebral and Cardiovascular Center Research Institute, Osaka, Japan

ARTICLE INFO

Article history:
Received 15 January 2010
Received in revised form 1 April 2010
Accepted 9 April 2010

Keywords:
Acetylcholine
Cardiac microdialysis
Vagal stimulation
Rabbits

ABSTRACT

Although large conductance Ca^{2+}-activated K^+ (BK) channels play an important role in determining vascular tone, their role in the efferent cardiac vagal system remains to be elucidated. In anesthetized rabbits ($n=9$), acetylcholine (ACh) was measured at the right atrium near the sinoatrial node by a cardiac microdialysis technique, and the ACh release in response to electrical stimulation of the cervical preganglionic vagal nerves was examined. Local administration of a BK channel blocker iberiotoxin (2 μM) through a dialysis fiber increased the stimulation-induced ACh release from 7.6±2.7 to 9.0±3.2 nM ($P<0.05$). Addition of intravenous administration of iberiotoxin (0.11 mg/body) did not increase the stimulation-induced ACh release further (10.8±4.4 nM). These results indicate that the BK channels play an inhibitory role in the vagal ACh release to the sinoatrial node.

1. Introduction

Ca^{2+}-activated K^+ channels are located in the vicinity of voltage-dependent Ca^{2+} channels. Their activation induces outward efflux of K^+, leading to hyperpolarization of the plasma membrane and promoting closure of the voltage-dependent Ca^{2+} channels. Among the group of Ca^{2+}-activated K^+ channels, large conductance Ca^{2+}-activated K^+ channels, also designated as the "Big K" (BK) channels, are expressed in the plasma membrane of vascular smooth muscle cells and contribute to the regulation of vascular tone (Ledoux et al., 2006). The BK channels are also found on neural cells and play a critical role in shaping action potentials and modifying firing patterns (Pedarzani et al., 2000). Blockade of the BK channels by iberiotoxin enhanced presynaptic release of acetylcholine (ACh) and postsynaptic release of catecholamine in the rat adrenal medulla during electrical stimulation of the splanchnic nerve, suggesting an inhibitory role of the BK channels in the physiological catecholamine release from the adrenal medulla (Akiyama et al., 2010). The role of the BK channels in the efferent vagal system in controlling the heart, however, remains to be elucidated. If the BK channels limit Ca^{2+} entry through the voltage-dependent Ca^{2+} channels in the preganglionic and/or postganglionic vagal nerve terminals, blockade of the BK channels by iberiotoxin would enhance the ACh release in response to electrical stimulation of the preganglionic vagal nerve. A recent development of a cardiac microdialysis technique in the in vivo rabbit right atrium has enabled direct monitoring of vagal ACh release to the sinoatrial node (Shimizu et al., 2009). This technique was used to examine the role of the BK channels in the efferent cardiac vagal system.

2. Materials and methods

Animal care was conducted in accordance with the *Guiding Principles for the Care and Use of Animals in the Field of Physiological Sciences*, which has been approved by the Physiological Society of Japan. All experimental protocols were reviewed and approved by the Animal Subjects Committee at the National Cerebral and Cardiovascular Center. Nine Japanese white rabbits weighing 2.3 kg to 3.0 kg were anesthetized via intravenous administration of pentobarbital sodium (30–35 mg/kg) through a marginal ear vein. A tracheal tube was inserted through a midline cervical incision. The animal was ventilated mechanically with room air mixed with oxygen through the tracheal tube. The anesthesia was maintained using a continuous intravenous infusion of urethane (125 mg/kg h^{-1}) and α-chloralose (20 mg/kg h^{-1}) through a catheter inserted into the right femoral vein. Mean arterial pressure (AP) was measured by a biological amplifier unit 2238 (San-ei, Japan) using a fluid-filled transducer (BD DTXPlus, Becton, Dickinson and Company) connected to a catheter inserted into the right femoral artery. Heart rate (HR) was derived from an electrocardiogram. Through a midline thoracotomy, the right thymus was removed. A main branch of the right cardiac sympathetic nerve was sectioned to reduce a possible

* Corresponding author. Department of Cardiovascular Dynamics, National Cerebral and Cardiovascular Center Research Institute, 5-7-1 Fujishirodai, Suita, Osaka 565-8565, Japan. Tel.: +81 6 6833 5012 x 2427; fax: +81 6 6835 5403.
E-mail address: torukawa@res.ncvc.go.jp (T. Kawada).

1566-0702/$ – see front matter © 2010 Elsevier B.V. All rights reserved.
doi:10.1016/j.autneu.2010.04.003

sympatho-vagal interaction in the ACh release. After incising the pericardium, a dialysis probe was implanted within the right atrial wall near the junction with the superior vena cava where the sinoatrial node resides (Shimizu et al., 2009). Bilateral vagal nerves were exposed and sectioned at the neck. A pair of platinum electrodes was attached to each sectioned nerve to stimulate the efferent vagal nerve. The dialysis probe was examined postmortem to confirm that it did not penetrate into the atrial cavity.

Acetylcholine was measured in the dialysate as an index of interstitial ACh concentrations. A dialysis fiber (outer diameter, 310 μm; inner diameter, 200 μm; PAN-1200, 50,000-Da molecular-weight cutoff, Asahi Chemical, Japan) was glued at both ends to polyethylene tubes (length, 25 cm; outer diameter, 500 μm; inner diameter, 200 μm) (Akiyama et al., 1994, Shimizu et al., 2009). The end of the polyethylene tube was enlarged by a dulled needle so that the dialysis fiber could be inserted. The exposed fiber length was 4 mm. The dialysis probe was perfused at a rate of 2 μl/min with Ringer solution containing a cholinesterase inhibitor eserine (100 μM). The amount of ACh in the dialysate was measured using a high-performance liquid chromatography system with electrochemical detection (Eicom, Japan) adjusted to measure low concentrations of ACh (Shimizu et al., 2009).

Two hours after the probe implantation, 10-minute dialysate samples were collected under control conditions, before and during bilateral vagal stimulation (10 V, 1-ms pulse width, 10 Hz). The actual dialysate sampling lagged behind a given collection period by 5 min taking into account the dead space volume between the dialysis membrane and collecting tube. After collecting the control data, the perfusate was replaced with the one containing iberiotoxin (2 μM). The local iberiotoxin administration (Ib_{Local}) is considered to affect vagal nerve terminals in the vicinity of the dialysis fiber. The dose was 40 times higher than that used in the in vitro experimental settings (Pedarzani et al., 2000), taking into account the distribution across the dialysis fiber. According to a previous study in rats (Akiyama et al., 2010), local administration of iberiotoxin at half dose (1 μM) significantly enhanced presynaptic ACh release in response to splanchnic nerve stimulation. Thirty minutes after the initiation of Ib_{Local}, 10-minute dialysate samples were collected before and during bilateral vagal stimulation. Next, iberiotoxin was administered intravenously (0.11 mg/body or 37–48 μg/kg, bolus) while continuing the local iberiotoxin administration. The dose was determined based on a previous study in rats (Meade, 1998) in which intravenous administration of iberiotoxin at approximately half dose (20 μg/kg) significantly blocked BK channels. The local plus intravenous iberiotoxin administration (Ib_{L+IV}) is considered to affect both preganglionic and postganglionic vagal nerve terminals. Ten minutes later, 10-minute dialysate samples were collected before and during bilateral vagal stimulation.

In order to check that a locally administered agent did not reach the vagal ganglia, a supplemental protocol was performed at the end of the experiment in five out of the nine rabbits as follows. The perfusate was replaced with the one containing a ganglionic blocker hexamethonium bromide (100 μM in one rabbit and 1 mM in four rabbits). Thirty minutes later, 10-minute dialysate samples were collected before and during bilateral vagal stimulation.

All data are presented as mean and SE values. Dialysate ACh concentrations were compared among three conditions of control, Ib_{Local} and Ib_{L+IV}, using the Friedman test based on ranks, followed by the rank-sum version of the Student–Newman–Keuls test for all pairwise comparisons (Glantz, 2002). AP and HR were measured just before and at 5 min of the 10-minute bilateral vagal stimulation. The AP and HR data were compared among the three conditions using repeated-measures analysis of variance followed by the parametric version of the Student–Newman–Keuls test (Glantz, 2002). In all of the statistical analyses, differences were considered significant when $P<0.05$.

3. Results

Baseline ACh measured before vagal stimulation did not differ significantly among the three conditions (Fig. 1A, left). Vagal stimulation-induced ACh release was significantly enhanced during the Ib_{Local} (118 ± 5% of the control) and Ib_{L+IV} conditions (129 ± 8% of the control) (Fig. 1A, right). There was no significant difference in the stimulation-induced ACh recovery between the Ib_{Local} and Ib_{L+IV} conditions.

Baseline HR measured before vagal stimulation did not differ significantly among the three conditions (Fig. 1B, left). The stimulation-induced bradycardia was augmented during the Ib_{L+IV} but not the Ib_{Local} conditions compared to the control conditions (Fig. 1B, right).

Baseline AP measured before vagal stimulation did not differ significantly among the three conditions (Fig. 1C, left). AP during vagal stimulation was significantly higher during the Ib_{L+IV} conditions compared to that under the control or Ib_{Local} conditions (Fig. 1C, right).

In the supplemental protocol of local hexamethonium administration, the ACh concentration was 3.3 ± 1.1 nM before vagal stimulation. Bilateral vagal stimulation increased the ACh levels in all of the 5 rabbits to 10.9 ± 7.3 nM ($P<0.05$, one-tailed signed test).

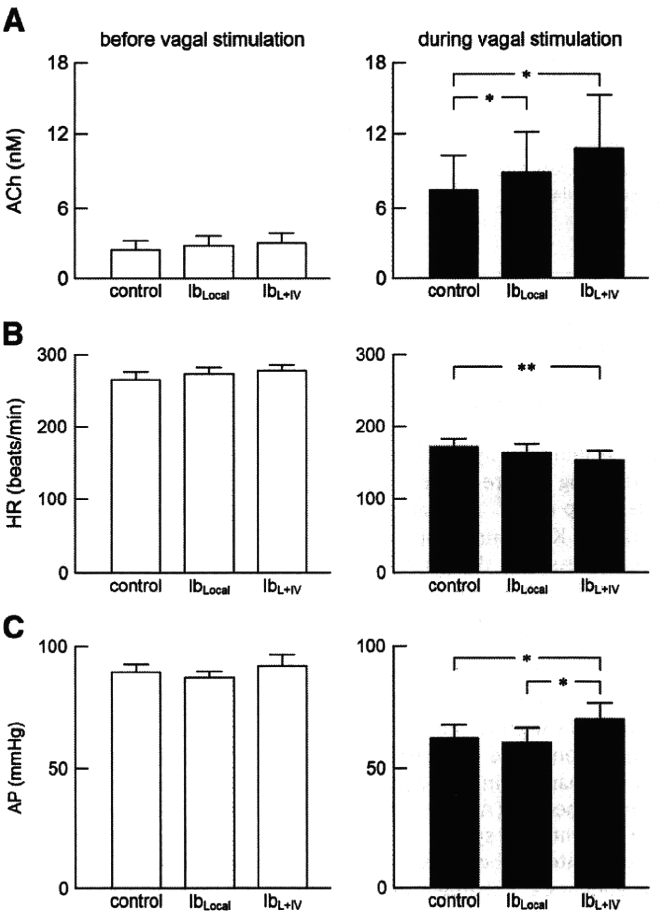

Fig. 1. A: Dialysate acetylcholine (ACh) concentrations under conditions of control, local iberiotoxin administration (Ib_{Local}) and local plus intravenous iberiotoxin administration (Ib_{L+IV}), before (left panel) and during (right panel) bilateral preganglionic vagal stimulation. Ib_{Local} and Ib_{L+IV} significantly increased the vagal stimulation-induced ACh release. B: Heat rate (HR) measured before (left panel) and during (right panel) vagal stimulation. Ib_{L+IV} significantly decreased the HR during vagal stimulation compared to that under control conditions. C: Arterial pressure (AP) measured before (left panel) and during (right panel) vagal stimulation. Ib_{L+IV} significantly increased the AP during vagal stimulation compared to that under the control and Ib_{Local} conditions. Values are mean and mean + SE. $^{*}P<0.05$ and $^{**}P<0.01$.

4. Discussion

Ib_{Local} significantly increased the vagal stimulation-induced ACh release, suggesting that the BK channels play an inhibitory role in the efferent cardiac vagal system (Fig. 1A, right). In a previous study, intravenous administration of hexamethonium bromide completely blocked the vagal stimulation-induced ACh release (Shimizu et al., 2009). In the present study, locally administered hexamethonium bromide is considered to have spread beyond the distribution of locally administered iberiotoxin because of the higher concentration (100 μM or 1 mM vs. 2 μM) and the smaller molecular weight (362.2 vs. 4232.0). Nevertheless, the locally administered hexamethonium bromide did not block the vagal stimulation-induced ACh release, suggesting that the locally administered pharmacological agents failed to reach the vagal ganglia. Therefore, the enhancement of the vagal stimulation-induced ACh release by Ib_{Local} may be attributable to the blockade of the BK channels at the postganglionic vagal nerve terminals.

Under experimental settings similar to the present study, the ACh release at the sinoatrial node can be increased more than 7 times higher during 40-Hz vagal stimulation than during 10-Hz vagal stimulation (Shimizu et al., 2009), suggesting that there remained a sufficient margin for the postganglionic vagal nerve to increase its activity to release ACh when the preganglionic vagal nerve was stimulated at 10 Hz. Under the Ib_{L+IV} conditions, the BK channels are assumed to be blocked at both the preganglionic and postganglionic vagal nerve terminals. If the BK channels limited the preganglionic ACh release to a considerable extent, Ib_{L+IV} could increase the postganglionic vagal nerve activity in response to the preganglionic vagal nerve stimulation. The stimulation-induced ACh release, however, did not differ statistically between the Ib_{Local} and Ib_{L+IV} conditions, suggesting that the inhibitory role of the BK channels at the preganglionic vagal nerve terminals, if any, did not surpass that at the postganglionic vagal nerve terminals.

Although vagi were sectioned at the neck, ACh was detected before vagal stimulation (Fig. 1A, left). In contrast to the vagal stimulation-induced ACh release, the basal ACh release was not affected significantly by Ib_{Local} or Ib_{L+IV}. According to a study using the isolated rat atrium (Abramochkin et al., 2010), a non-quantal ACh release, probably via the choline uptake system, contributes to the basal ACh release from the vagal nerve terminals. It is likely that the blockade of BK channels did not affect the baseline ACh concentrations significantly because the voltage-dependent Ca^{2+} channels contributed little to the basal ACh release.

HR during vagal stimulation under the Ib_{Local} conditions did not differ significantly from that observed under the control conditions (Fig. 1B, right). Presuming that Ib_{Local} affected the ACh release only in the vicinity of the dialysis fiber, not all the vagal nerve fibers innervating the sinoatrial node might have been affected by iberiotoxin. In contrast, HR during vagal stimulation under the Ib_{L+IV} conditions was significantly lower than that observed under the control conditions, suggesting perhaps that the systemically administered iberiotoxin reached a larger portion of the vagal fibers innervating the sinoatrial node.

Ib_{Local} did not affect AP both before and during vagal stimulation (Fig. 1C). Ib_{L+IV} did not increase AP but reduced the vagally mediated hypotension. Possible explanation is as follows. Vagal stimulation significantly decreased AP, possibly via the suppression of cardiac function. Resultantly, the systemic sympathetic system might have been activated through the arterial baroreflex during vagal stimulation. Blockade of the BK channels enhances the vasoconstriction of vascular smooth muscles (Ledoux et al., 2006) and the catecholamine release from the adrenal medulla (Akiyama et al., 2010), resulting in the higher AP during vagal stimulation under the Ib_{L+IV} conditions. The moderation of the vagally mediated hypotension may also have resulted from a more efficient baroreflex response under the Ib_{L+IV} conditions.

There are several limitations in the present study. First, eserine was added to the perfusate to improve the recovery of ACh. Although the inhibition of cholinesterase activity may have affected the ACh kinetics, its influence should have been consistent throughout the protocols. Second, vagal stimulation intensity was selected to limit the hypotensive response and maintain the AP at 60 mm Hg or higher under the control conditions. Based on the results of unilateral vagal stimulation in a previous study (Shimizu et al., 2009), increasing the stimulation frequency would further increase the ACh release. The inhibitory effects of the BK channels on the efferent cardiac vagal system could be different under such an intense vagal stimulation. Finally, the present results do not preclude that the BK channels are on the post-junctional sinus nodal cells or on the cross-inhibitory adrenergic nerves. Nevertheless, the BK channels on the sinus nodal cells or on the adrenergic nerves do not well account for the present results as follows. Although the BK channels on the sinus nodal cells may have modified the HR response and caused possible dissociation between the ACh recovery and the degree of bradycardia, they may not explain the enhanced ACh recovery after the iberiotoxin administration. With respect to the BK channels on the cross-inhibitory adrenergic nerves, if the BK channels are inhibitory to catecholamine release, iberiotoxin is expected to enhance the catecholamine release, antagonizing rather than promoting the vagal ACh release during vagal stimulation. Further studies are needed to confirm these speculations.

In conclusion, blockade of the BK channels by iberiotoxin enhanced the vagal stimulation-induced ACh release and bradycardia, suggesting an inhibitory role of the BK channels in the efferent cardiac vagal system. The inhibitory role of the BK channels at the vagal ganglia did not seem to surpass that at the postganglionic vagal nerve terminals. Although a potential use of selective BK channel openers is expected as vasodilators for vascular smooth muscle dysfunction (Ledoux et al., 2006), there is a possibility that BK channel openers limit vagal effect on the heart, which can be undesirable in certain cardiovascular diseases in which improved vagal function would be helpful.

Acknowledgments

This study was supported by Health and Labour Sciences Research Grants (H18-nano-Ippan-003, H19-nano-Ippan-009, H20-katsudo-Shitei-007, and H21-nano-Ippan-005) from the Ministry of Health, Labour and Welfare of Japan; by a Grant-in-Aid for Scientific Research (No. 20390462) from the Ministry of Education, Culture, Sports, Science and Technology of Japan; and by the Industrial Technology Research Grant Program from the New Energy and Industrial Technology Development Organization (NEDO) of Japan.

References

Abramochkin, D.V., Nurullin, L.F., Borodinova, A.A., Tarasova, N.V., Sukhova, G.S., Nikolsky, E.E., Rosenshtraukh, L.V., 2010. Non-quantal release of acetylcholine from parasympathetic nerve terminals in the right atrium of rats. Exp. Physiol. 95 (2), 265–273.

Akiyama, T., Yamazaki, T., Kawada, T., Shimizu, S., Sugimachi, M., Shirai, M., 2010. Role of Ca^{2+}-activated K^+ channels in catecholamine release from in vivo rat adrenal medulla. Neurochem. Int. 56, 263–269.

Akiyama, T., Yamazaki, T., Ninomiya, I., 1994. In vivo detection of endogenous acetylcholine release in cat ventricles. Am. J. Physiol. 266 (3 Pt 2), H854–H860.

Glantz, S.A., 2002. Primer of Biostatistics, 5th ed. McGraw-Hill, New York.

Ledoux, J., Werner, M.E., Brayden, J.E., Nelson, M.T., 2006. Calcium-activated potassium channels and the regulation of vascular tone. Physiol. 21, 69–79.

Meade, C.J., 1998. The mechanism by which epinastine stops an adenosine analog from contracting BDE rat airways. Am. J. Respir. Crit. Care Med. 157, 522–530.

Pedarzani, P., Kulik, A., Müller, M., Ballanyi, K., Stocker, M., 2000. Molecular determinants of Ca^{2+}-dependent K^+ channel function in rat dorsal vagal neurones. J. Physiol. 527, 283–290.

Shimizu, S., Akiyama, T., Kawada, T., Shishido, T., Yamazaki, T., Kamiya, A., Mizuno, M., Sano, S., Sugimachi, M., 2009. In vivo direct monitoring of vagal acetylcholine release to the sinoatrial node. Auton. Neurosci. 148, 44–49.

Am J Physiol Heart Circ Physiol 298: H1966–H1975, 2010.
First published March 26, 2010; doi:10.1152/ajpheart.00340.2009.

Parallel resetting of arterial baroreflex control of renal and cardiac sympathetic nerve activities during upright tilt in rabbits

Atsunori Kamiya, Toru Kawada, Masaki Mizuno, Shuji Shimizu, and Masaru Sugimachi

Department of Cardiovascular Dynamics, National Cardiovascular Centre Research Institute, Suita, Japan

Submitted 8 April 2009; accepted in final form 23 March 2010

Kamiya A, Kawada T, Mizuno M, Shimizu S, Sugimachi M. Parallel resetting of arterial baroreflex control of renal and cardiac sympathetic nerve activities during upright tilt in rabbits. *Am J Physiol Heart Circ Physiol* 298: H1966–H1975, 2010. First published March 26, 2010; doi:10.1152/ajpheart.00340.2009.—Since humans are under ceaseless orthostatic stress, the mechanisms to maintain arterial pressure (AP) against gravitational fluid shift are important. As one mechanism, it was reported that upright tilt reset baroreflex control of renal sympathetic nerve activity (SNA) to a higher SNA in anesthetized rabbits. In the present study, we tested the hypothesis that upright tilt causes a parallel resetting of baroreflex control of renal and cardiac SNAs in anesthetized rabbits. In anesthetized rabbits (n = 8, vagotomized and aortic denervated) with 0° supine and 60° upright tilt postures, renal and cardiac SNAs were simultaneously recorded while isolated intracarotid sinus pressure (CSP) was increased stepwise from 40 to 160 mmHg with increments of 20 mmHg. Upright tilt shifted the reverse-sigmoidal curve of the CSP-SNA relationship to higher SNA similarly in renal and cardiac SNAs. Although upright tilt increased the maximal gain, the response range and the minimum value of SNA, the curves were almost superimposable in these SNAs regardless of postures. Scatter plotting of cardiac SNA over renal SNA during the stepwise changes in CSP was close to the line of identity in 0° supine and 60° upright tilt postures. In addition, upright tilt also shifted the reverse-sigmoidal curve of the CSP-heart rate relationship to a higher heart rate, with increases in the maximal gain and the response range. In conclusion, upright posture caused a resetting of arterial baroreflex control of SNA similarly in renal and cardiac SNAs in anesthetized rabbits.

blood pressure; orthostasis; sympathetic nervous system

SINCE HUMANS ARE UNDER CEASELESS orthostatic stress, the mechanisms to maintain arterial pressure (AP) against gravitational fluid shift are greatly important. During standing, a gravitational fluid shift directed toward the lower part of the body (such as the abdominal vascular bed and lower limbs) will cause severe postural hypotension if not counteracted by compensatory mechanisms (15). Arterial baroreflexes have been considered to be the major compensatory mechanism (1, 13, 15), since denervation of baroreceptor afferents causes profound postural hypotension (16). In addition, we (8) recently reported that upright tilt resets baroreflex control of sympathetic nerve activity (SNA) to higher SNA. The resetting doubles SNA, compensates for the reduced pressor responses of cardiovascular organs to SNA during gravitational stress, and contributes to prevent postural hypotension. However, since the study recorded only renal SNA, it remains unknown whether upright tilt resets arterial baroreflex control of SNA innervating cardiovascular organs (i.e., the heart) other than the kidney. Since cardiac SNA has a critical role in circulation, baroreflex control of cardiac SNA during orthostatic stress is of importance.

Accordingly, in the present study, we tested the hypothesis that upright tilt causes a parallel resetting of arterial baroreflex control of renal and cardiac SNAs in anesthetized rabbits. Since total baroreflex is a closed-loop negative feedback system that senses baroreceptor pressure and controls AP, and since the baroreflex control of SNA (from baroreceptor pressure input to SNA) is a subsystem of the total baroreflex system, it is difficult to isolate the baroreflex control of SNA from the total system in the baroreflex closed-loop condition (16). Therefore, we opened the baroreflex feedback loop by vascularly isolating the carotid sinus region and loaded artificial stepwise intracarotid sinus pressure (CSP) in anesthetized rabbits. By recording renal and cardiac SNAs simultaneously, we investigated static characteristics of baroreflex control of these SNAs (CSP-SNA relationship) in 0° and 60° upright tilt postures.

METHODS

Animals, preparation, and measurements. Japanese White rabbits weighing 2.4–3.3 kg were used. Animals were cared for in strict accordance with the "Guiding Principles for the Care and Use of Animals in the Field of Physiological Science" approved by the Physiological Society of Japan.

Animals (n = 8) were initially anesthetized by intravenous injection (2 ml/kg) of a mixture of urethane (250 mg/ml) and α-chloralose (40 mg/ml). Anesthesia was maintained by continuously infusing the anesthetics at a rate of 0.33 $ml \cdot kg^{-1} \cdot h^{-1}$ using a syringe pump (CFV-3200; Nihon Kohden, Tokyo, Japan). The rabbits were mechanically ventilated with oxygen-enriched room air. Bilateral carotid sinuses were isolated vascularly from the systemic circulation by ligating the internal and external carotid arteries and other small branches originating from the carotid sinus regions. The isolated carotid sinuses were filled with warmed physiological saline, preequilibrated with atmospheric air, through catheters inserted via the common carotid arteries. The intracarotid sinus pressure (CSP) was controlled by a servo-controlled piston pump (model ET-126A; Labworks, Costa Mesa, CA). Bilateral vagal and aortic depressor nerves were sectioned in the middle of the neck region to eliminate reflexes from the cardiopulmonary region and the aortic arch. The systemic AP was measured using a high-fidelity pressure transducer (Millar Instruments, Houston, TX) inserted retrograde from the right common carotid artery below the isolated carotid sinus region. Heart rate (HR) was measured with a cardiotachometer (model N4778; San-ei, Tokyo, Japan).

Body temperature was maintained at around 38°C with a heating pad. The left renal sympathetic nerve was exposed retroperitoneally, and the left cardiac sympathetic nerve was exposed through a middle thoracotomy. A pair of stainless steel wire electrodes (Bioflex wire AS633; Cooner Wire) was hooked onto each of these nerves to record renal and cardiac SNAs. The nerve fibers peripheral to electrodes were ligated securely and crushed to eliminate afferent signals. The nerve

Address for reprint requests and other correspondence: A. Kamiya, Dept. of Cardiovascular Dynamics, National Cardiovascular Centre Research Institute, Suita 565-8565, Japan (e-mail: kamiya@ri.ncvc.go.jp).

and electrodes were covered with a mixture of silicone gel (silicon low viscosity, Kwik-Sil; World Precision Instruments, Sarasota, FL) to insulate and immobilize the electrodes. The preamplified SNA signals were band-pass filtered at 150–1,000 Hz. These nerve signals were full-wave rectified and low-pass filtered with a cutoff frequency of 30 Hz to quantify the nerve activity. After the experiment, an intravenous infusion of hexamethonium bromide (6 mg/kg) abolished the SNA signals, indicating that the signals recorded were postganglionic SNA.

Protocols. After the preparation, the animal was maintained in a 0° supine posture on a tilt bed. To stabilize the posture, the head was fixed full-frontal to the bed by strings, and the body and legs were rigged up in a clothes-like bag. Bilateral CSP was artificially controlled independently of systemic AP. First, actual operating pressure and SNAs under baroreflex closed-loop conditions in the 0° supine posture were obtained. The animal was kept in the 0° supine posture for 10 min while CSP was matched with systemic AP via the servo-controlled piston pump.

Second, the static characteristics of the sympathetic baroreflex system were estimated in the 0° position under baroreflex open-loop conditions. The animal was kept in the 0° supine posture while CSP was decreased to 40 mmHg and then increased stepwise from 40 to 160 mmHg in increments of 20 mmHg. Each CSP step was maintained for 60 s.

Third, actual operating pressure and SNAs under baroreflex closed-loop conditions in the 60° upright tilt position were obtained. The animal was kept supine for 10 min and then tilted upright to 60° within 10 s by inclining the tilt bed to 60° and dropping the lower regions of the rabbit with the fulcrum set at the level of the carotid sinus. The 60° upright posture was maintained for 10 min. CSP was matched with systemic AP via the servo-controlled piston pump. Since the clothes-like bag stabilized the posture of the animals, there was no additional mechanical movement that reduced the quality of measurements. The position of the head remained almost fixed during the tilt to minimize vestibular stimulation. Last, the static characteristics of the sympathetic baroreflex system were estimated during the 60° upright tilt posture. CSP was increased stepwise from 40 to 160 mmHg similarly to the experiment in the 0° position. These SNAs and AP were recorded at a 200-Hz sampling rate using a 12-bit analog-to-digital converter and stored on the hard disk of a dedicated laboratory computer system for later analysis.

Data analysis. The SNA signals were normalized by the following steps. First, for each type of SNA, 0 arbitrary unit (a.u.) was assigned to the postmortem noise level. Second, 100 a.u. were assigned to the average of actual operating SNA values during baseline period in 0° positions. Last, the other SNA signals were then normalized to these values in each experiment.

These SNA and HR values were averaged for the last 10 s of each CSP level. The static relationships between CSP and SNA and between CSP and HR were parameterized by two widely used traditional models (nonlinear reverse-sigmoidal curve, linear regression line), although both models have limited abilities to reproduce the actual data. In the former case, the data were parameterized by a four-parameter logistic equation model as follows:

$$Y = P_4 + \frac{P_1}{1 + \exp[P_2(CSP - P_3)]} \quad (1)$$

where Y is SNA or HR, P_1 is the response range of Y (i.e., the difference between the maximum and minimum values of Y), P_2 is the coefficient of gain, P_3 is the midpoint CSP of the logistic function, and P_4 is the minimum value of Y. We calculated the instantaneous gain

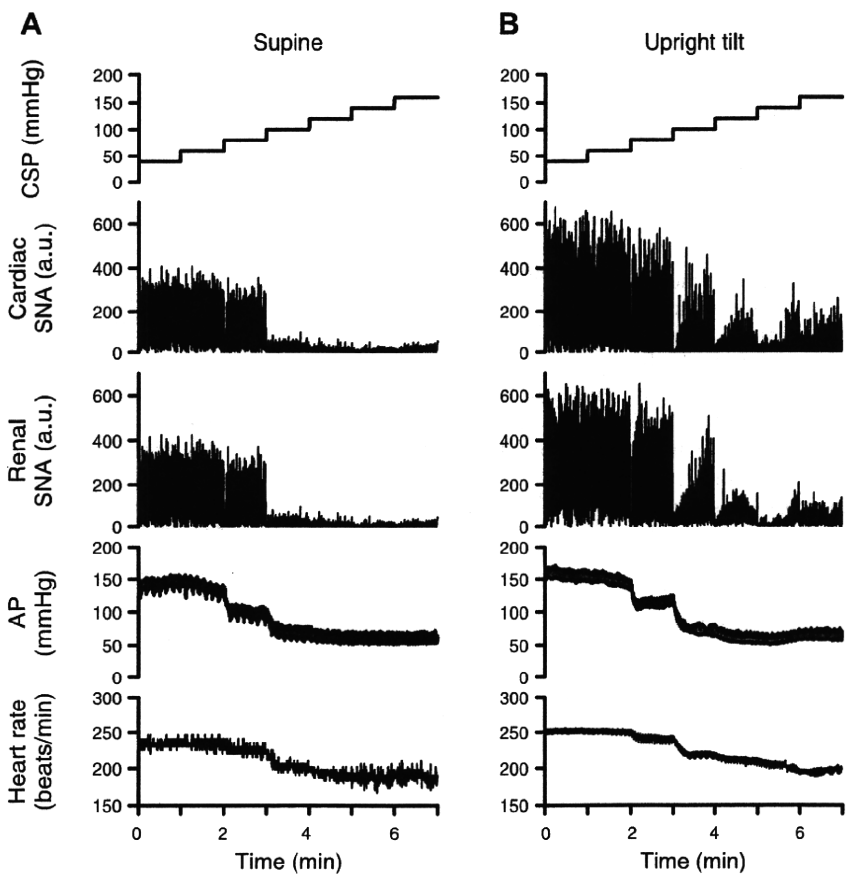

Fig. 1. Representative time series of renal and cardiac sympathetic nerve activities (SNAs) and arterial pressure (AP) in response to a stepwise increase in intracarotid sinus pressure (CSP) in 0° supine (*A*) and 60° upright tilt postures (*B*) obtained from 1 animal. Each CSP step was maintained for 1 min. All data were sampled at 10 Hz. In both SNAs, increasing CSP decreased SNAs in both postures, but upright tilt increased SNAs at all CSP levels. a.u., Arbitrary unit.

Am J Physiol Heart Circ Physiol 298: H1966–H1975, 2010.
First published March 26, 2010; doi:10.1152/ajpheart.00340.2009.

Parallel resetting of arterial baroreflex control of renal and cardiac sympathetic nerve activities during upright tilt in rabbits

Atsunori Kamiya, Toru Kawada, Masaki Mizuno, Shuji Shimizu, and Masaru Sugimachi

Department of Cardiovascular Dynamics, National Cardiovascular Centre Research Institute, Suita, Japan

Submitted 8 April 2009; accepted in final form 23 March 2010

Kamiya A, Kawada T, Mizuno M, Shimizu S, Sugimachi M. Parallel resetting of arterial baroreflex control of renal and cardiac sympathetic nerve activities during upright tilt in rabbits. *Am J Physiol Heart Circ Physiol* 298: H1966–H1975, 2010. First published March 26, 2010; doi:10.1152/ajpheart.00340.2009.—Since humans are under ceaseless orthostatic stress, the mechanisms to maintain arterial pressure (AP) against gravitational fluid shift are important. As one mechanism, it was reported that upright tilt reset baroreflex control of renal sympathetic nerve activity (SNA) to a higher SNA in anesthetized rabbits. In the present study, we tested the hypothesis that upright tilt causes a parallel resetting of baroreflex control of renal and cardiac SNAs in anesthetized rabbits. In anesthetized rabbits ($n = 8$, vagotomized and aortic denervated) with 0° supine and 60° upright tilt postures, renal and cardiac SNAs were simultaneously recorded while isolated intracarotid sinus pressure (CSP) was increased stepwise from 40 to 160 mmHg with increments of 20 mmHg. Upright tilt shifted the reverse-sigmoidal curve of the CSP-SNA relationship to higher SNA similarly in renal and cardiac SNAs. Although upright tilt increased the maximal gain, the response range and the minimum value of SNA, the curves were almost superimposable in these SNAs regardless of postures. Scatter plotting of cardiac SNA over renal SNA during the stepwise changes in CSP was close to the line of identity in 0° supine and 60° upright tilt postures. In addition, upright tilt also shifted the reverse-sigmoidal curve of the CSP-heart rate relationship to a higher heart rate, with increases in the maximal gain and the response range. In conclusion, upright posture caused a resetting of arterial baroreflex control of SNA similarly in renal and cardiac SNAs in anesthetized rabbits.

blood pressure; orthostasis; sympathetic nervous system

SINCE HUMANS ARE UNDER CEASELESS orthostatic stress, the mechanisms to maintain arterial pressure (AP) against gravitational fluid shift are greatly important. During standing, a gravitational fluid shift directed toward the lower part of the body (such as the abdominal vascular bed and lower limbs) will cause severe postural hypotension if not counteracted by compensatory mechanisms (15). Arterial baroreflexes have been considered to be the major compensatory mechanism (1, 13, 15), since denervation of baroreceptor afferents causes profound postural hypotension (16). In addition, we (8) recently reported that upright tilt resets baroreflex control of sympathetic nerve activity (SNA) to higher SNA. The resetting doubles SNA, compensates for the reduced pressor responses of cardiovascular organs to SNA during gravitational stress, and contributes to prevent postural hypotension. However, since the study recorded only renal SNA, it remains unknown whether upright tilt resets arterial baroreflex control of SNA innervating cardiovascular organs (i.e., the heart) other than the kidney. Since cardiac SNA has a critical role in circulation, baroreflex control of cardiac SNA during orthostatic stress is of importance.

Accordingly, in the present study, we tested the hypothesis that upright tilt causes a parallel resetting of arterial baroreflex control of renal and cardiac SNAs in anesthetized rabbits. Since total baroreflex is a closed-loop negative feedback system that senses baroreceptor pressure and controls AP, and since the baroreflex control of SNA (from baroreceptor pressure input to SNA) is a subsystem of the total baroreflex system, it is difficult to isolate the baroreflex control of SNA from the total system in the baroreflex closed-loop condition (16). Therefore, we opened the baroreflex feedback loop by vascularly isolating the carotid sinus region and loaded artificial stepwise intracarotid sinus pressure (CSP) in anesthetized rabbits. By recording renal and cardiac SNAs simultaneously, we investigated static characteristics of baroreflex control of these SNAs (CSP-SNA relationship) in 0° and 60° upright tilt postures.

METHODS

Animals, preparation, and measurements. Japanese White rabbits weighing 2.4–3.3 kg were used. Animals were cared for in strict accordance with the "Guiding Principles for the Care and Use of Animals in the Field of Physiological Science" approved by the Physiological Society of Japan.

Animals ($n = 8$) were initially anesthetized by intravenous injection (2 ml/kg) of a mixture of urethane (250 mg/ml) and α-chloralose (40 mg/ml). Anesthesia was maintained by continuously infusing the anesthetics at a rate of 0.33 $ml \cdot kg^{-1} \cdot h^{-1}$ using a syringe pump (CFV-3200; Nihon Kohden, Tokyo, Japan). The rabbits were mechanically ventilated with oxygen-enriched room air. Bilateral carotid sinuses were isolated vascularly from the systemic circulation by ligating the internal and external carotid arteries and other small branches originating from the carotid sinus regions. The isolated carotid sinuses were filled with warmed physiological saline, preequilibrated with atmospheric air, through catheters inserted via the common carotid arteries. The intracarotid sinus pressure (CSP) was controlled by a servo-controlled piston pump (model ET-126A; Labworks, Costa Mesa, CA). Bilateral vagal and aortic depressor nerves were sectioned in the middle of the neck region to eliminate reflexes from the cardiopulmonary region and the aortic arch. The systemic AP was measured using a high-fidelity pressure transducer (Millar Instruments, Houston, TX) inserted retrograde from the right common carotid artery below the isolated carotid sinus region. Heart rate (HR) was measured with a cardiotachometer (model N4778; San-ei, Tokyo, Japan).

Body temperature was maintained at around 38°C with a heating pad. The left renal sympathetic nerve was exposed retroperitoneally, and the left cardiac sympathetic nerve was exposed through a middle thoracotomy. A pair of stainless steel wire electrodes (Bioflex wire AS633; Cooner Wire) was hooked onto each of these nerves to record renal and cardiac SNAs. The nerve fibers peripheral to electrodes were ligated securely and crushed to eliminate afferent signals. The nerve

Address for reprint requests and other correspondence: A. Kamiya, Dept. of Cardiovascular Dynamics, National Cardiovascular Centre Research Institute, Suita 565-8565, Japan (e-mail: kamiya@ri.ncvc.go.jp).

and electrodes were covered with a mixture of silicone gel (silicon low viscosity, Kwik-Sil; World Precision Instruments, Sarasota, FL) to insulate and immobilize the electrodes. The preamplified SNA signals were band-pass filtered at 150–1,000 Hz. These nerve signals were full-wave rectified and low-pass filtered with a cutoff frequency of 30 Hz to quantify the nerve activity. After the experiment, an intravenous infusion of hexamethonium bromide (6 mg/kg) abolished the SNA signals, indicating that the signals recorded were postganglionic SNA.

Protocols. After the preparation, the animal was maintained in a 0° supine posture on a tilt bed. To stabilize the posture, the head was fixed full-frontal to the bed by strings, and the body and legs were rigged up in a clothes-like bag. Bilateral CSP was artificially controlled independently of systemic AP. First, actual operating pressure and SNAs under baroreflex closed-loop conditions in the 0° supine posture were obtained. The animal was kept in the 0° supine posture for 10 min while CSP was matched with systemic AP via the servo-controlled piston pump.

Second, the static characteristics of the sympathetic baroreflex system were estimated in the 0° position under baroreflex open-loop conditions. The animal was kept in the 0° supine posture while CSP was decreased to 40 mmHg and then increased stepwise from 40 to 160 mmHg in increments of 20 mmHg. Each CSP step was maintained for 60 s.

Third, actual operating pressure and SNAs under baroreflex closed-loop conditions in the 60° upright tilt position were obtained. The animal was kept supine for 10 min and then tilted upright to 60° within 10 s by inclining the tilt bed to 60° and dropping the lower regions of the rabbit with the fulcrum set at the level of the carotid sinus. The 60° upright posture was maintained for 10 min. CSP was matched with systemic AP via the servo-controlled piston pump. Since the clothes-like bag stabilized the posture of the animals, there was no additional mechanical movement that reduced the quality of measurements. The position of the head remained almost fixed during the tilt to minimize vestibular stimulation. Last, the static characteristics of the sympathetic baroreflex system were estimated during the 60° upright tilt posture. CSP was increased stepwise from 40 to 160 mmHg similarly to the experiment in the 0° position. These SNAs and AP were recorded at a 200-Hz sampling rate using a 12-bit analog-to-digital converter and stored on the hard disk of a dedicated laboratory computer system for later analysis.

Data analysis. The SNA signals were normalized by the following steps. First, for each type of SNA, 0 arbitrary unit (a.u.) was assigned to the postmortem noise level. Second, 100 a.u. were assigned to the average of actual operating SNA values during baseline period in 0° positions. Last, the other SNA signals were then normalized to these values in each experiment.

These SNA and HR values were averaged for the last 10 s of each CSP level. The static relationships between CSP and SNA and between CSP and HR were parameterized by two widely used traditional models (nonlinear reverse-sigmoidal curve, linear regression line), although both models have limited abilities to reproduce the actual data. In the former case, the data were parameterized by a four-parameter logistic equation model as follows:

$$Y = P_4 + \frac{P_1}{1 + \exp[P_2(CSP - P_3)]} \quad (1)$$

where Y is SNA or HR, P_1 is the response range of Y (i.e., the difference between the maximum and minimum values of Y), P_2 is the coefficient of gain, P_3 is the midpoint CSP of the logistic function, and P_4 is the minimum value of Y. We calculated the instantaneous gain

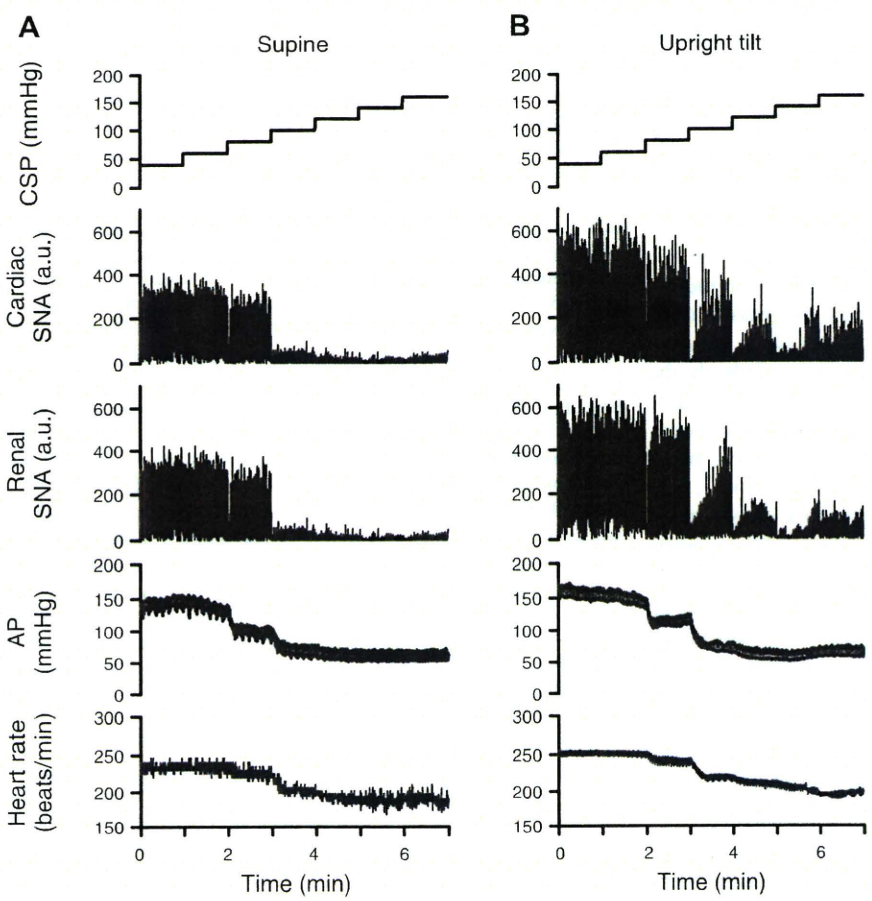

Fig. 1. Representative time series of renal and cardiac sympathetic nerve activities (SNAs) and arterial pressure (AP) in response to a stepwise increase in intracarotid sinus pressure (CSP) in 0° supine (*A*) and 60° upright tilt postures (*B*) obtained from 1 animal. Each CSP step was maintained for 1 min. All data were sampled at 10 Hz. In both SNAs, increasing CSP decreased SNAs in both postures, but upright tilt increased SNAs at all CSP levels. a.u., Arbitrary unit.

from the first derivative of the logistic function and the maximum gain (G_{max}) from $-P_1P_2/4$ at CSP = P_3.

Statistic analysis. All data are means ± SD. Effects of the upright tilt on baroreflex parameters were evaluated by repeated-measures analysis of variance. When the main effect was found to be significant, post hoc multiple comparisons were made using Scheffé's *F*-test to compare baroreflex controls between renal and cardiac SNAs (3). Differences were considered significant when $P < 0.05$.

RESULTS

Baroreflex control of renal and cardiac SNAs. Figure 1 shows the representative time series data obtained from one subject. The renal and cardiac SNAs similarly decreased in response to stepwise increase in CSP in the 0° supine posture (Fig. 1*A*). The 60° upright tilt increased these SNAs at each CSP level (Fig. 1*B*) compared with the supine posture.

Figure 2 shows the relationship between CSP and SNA in the same data as in Fig. 1*A*. In Fig. 2, these SNAs were averaged for the last 10 s of each CSP level to investigate the steady-state, not transient, response to a stepwise change in CSP. The 60° upright tilt increased renal (Fig. 2*A*) and cardiac SNAs (Fig. 2*C*) at all CSP levels compared with the supine posture. The renal SNA approximately matched the cardiac SNA at all CSP levels in the supine posture (Fig. 2*B*) and also in the upright tilt posture (Fig. 2*D*).

When the static relationship between CSP and each SNA was fitted to a nonlinear reverse-sigmoidal curve (Fig. 3), the r^2 value was ~0.95. The 60° upright tilt shifted the CSP-renal SNA curve upward to a higher SNA (Fig. 3*A*). Similarly, the upright tilt shifted the CSP-cardiac SNA curve (Fig. 3*C*) in the same manner as renal SNA. The CSP-renal SNA curve was almost superimposed on the CSP-cardiac SNA curve in the 0° supine (Fig. 3*B*) and upright tilt postures (Fig. 3*D*). However, the model was limited in reproducing the data, since the measured SNAs did not saturate at the CSP levels of 40–60 mmHg.

When the static relationship between CSP and each SNA was fitted to a linear regression line (Fig. 4), the r^2 value was 0.82–88, lower than when the nonlinear reverse-sigmoidal curve was used. The 60° upright tilt shifted the CSP-renal SNA (Fig. 4*A*) and the CSP-cardiac SNA lines (Fig. 4*C*) upward to the higher SNA levels. The CSP-renal SNA line was almost superimposed on the CSP-cardiac SNA line in the 0° supine (Fig. 4*B*) and upright tilt postures (Fig. 4*D*).

Averaged data from all animals showed that the 60° upright tilt increased renal (Fig. 5*A*) and cardiac SNAs (Fig. 5*B*) at all CSP levels compared with the 0° supine posture. The renal SNA almost matched the cardiac SNA at all CSP levels in the supine (Fig. 5*D*) and also in the upright tilt posture (Fig. 5*E*),

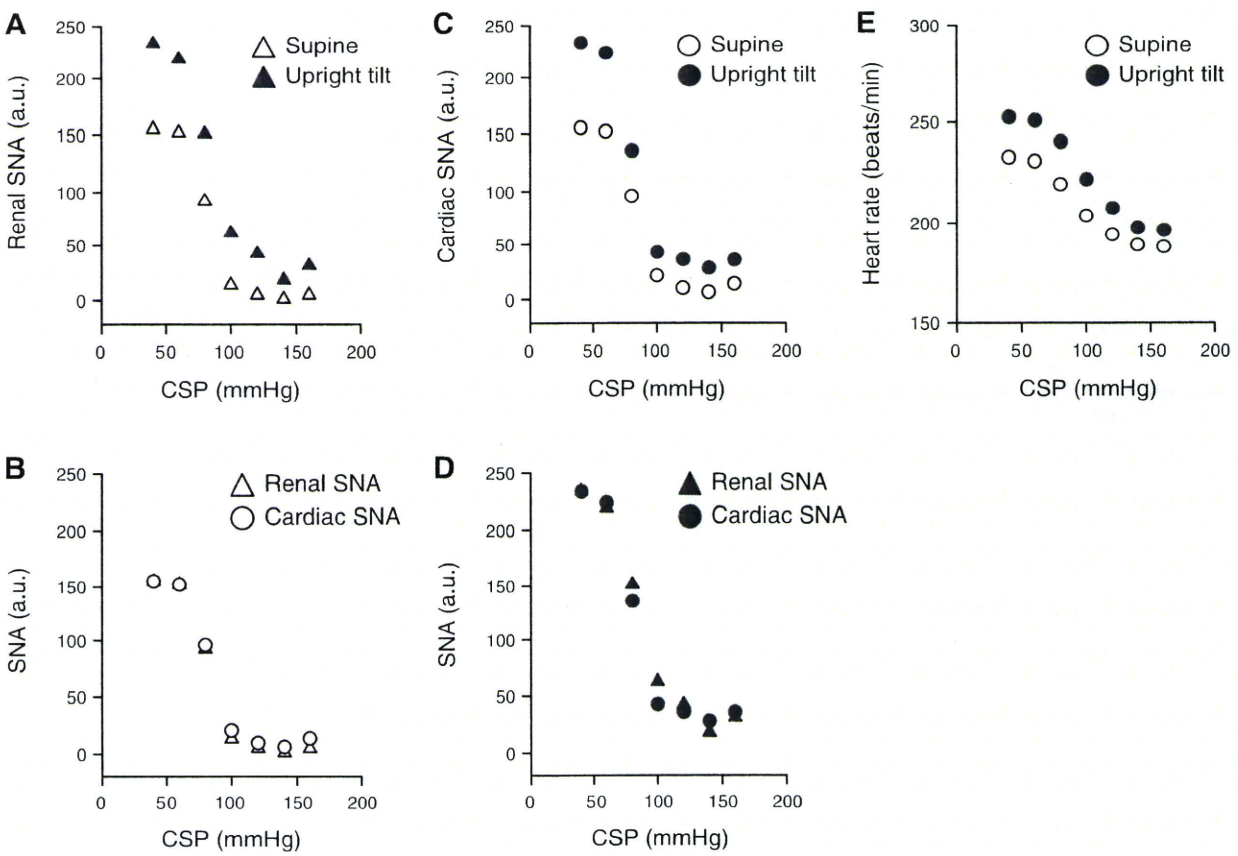

Fig. 2. Example of arterial baroreflex control of renal (*A*) and cardiac SNAs (*C*) and heart rate (HR; *E*). Data were obtained from the same animal studied in Fig. 1 and averaged for the last 10 s of each CSP level. Open and filled symbols show the data in the supine and 60° upright tilt postures, respectively. The upright tilt shifted the baroreflex control of SNA to a higher SNA similarly in the CSP-renal SNA (*A*) and CSP-cardiac SNA relationships (*C*). Data in *B* and *D* represent the superimposing of baroreflex control of SNA between renal and cardiac SNAs in both the supine and upright tilt postures, respectively. The upright tilt also shifted the baroreflex control of HR upward (*E*).

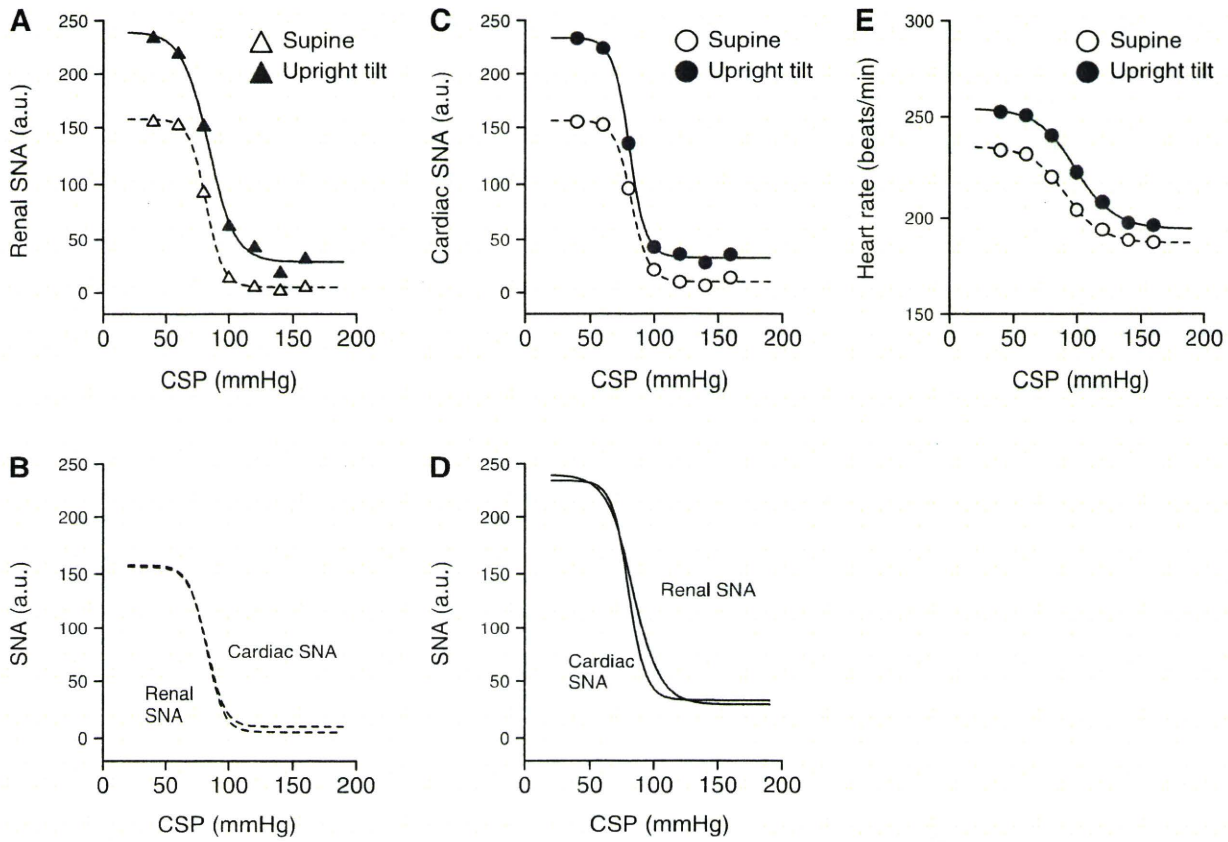

Fig. 3. Example of a model of the data shown in Fig. 2 using reverse-sigmoid 4-parameter logistic functions. Dotted and solid curves show the data in the supine and 60° upright tilt postures, respectively. The upright tilt shifted the baroreflex curves to a higher SNA similarly in renal (*A*) and cardiac SNAs (*C*). The curves were superimposed between these SNAs in the supine (*B*) and upright tilt postures (*D*). The upright tilt also shifted the baroreflex curve of HR upward (*E*).

indicating that 60° upright tilt shifted the CSP-SNA relationship upward by similar magnitudes in renal and cardiac SNAs.

When the static relationship between CSP and each SNA was fitted to a nonlinear reverse-sigmoidal curve (Fig. 6), the upright tilt shifted the CSP-SNA curve to higher SNA similarly in renal (Fig. 6*A*) and cardiac SNAs (Fig. 6*C*). The CSP-SNA relationship was almost superimposed between these SNAs in both the supine (Fig. 6*B*) and upright tilt postures (Fig. 4*D*). In both renal and cardiac SNAs, P_1 (the range of SNA response to CSP), P_4 (the minimum value of SNA), and the maximal gain (at the midpoint of the logistic function) were larger at upright tilt than supine posture (Table 1), whereas P_2 (the coefficient of gain) and P_3 (the midpoint CSP of the logistic function) were not different between postures (Table 1). In both postures, these parameters of P_{1-4} and maximal gain were similar in renal and cardiac SNAs (Table 1).

When the static relationship between CSP and each SNA was fitted to a linear regression line (Fig. 7), the upright tilt shifted the CSP-SNA line to higher SNA similarly in renal (Fig. 7*A*) and cardiac SNAs (Fig. 7*C*). It increased the slope of regression from -1.4 ± 0.3 to -1.8 ± 0.3 a.u./mmHg in renal SNA and from -1.4 ± 0.3 to -1.8 ± 0.4 a.u./mmHg in cardiac SNA. The CSP-SNA lines were almost superimposed on their SNAs in the 0° supine (Fig. 7*B*) and also the upright tilt posture (Fig. 7*D*). In both SNAs of all animals, the r^2 value was always lower (0.80–0.89) than when a nonlinear reverse-sigmoidal curve was used (0.92–0.97).

In addition, in both 0° supine and 60° upright tilt postures, scatter plotting of cardiac SNA over renal SNA was approximately close to the line of identity for each subject (Fig. 8A) and the pooled data from all subjects (Fig. 8*B*), indicating that these SNAs changed in parallel in response to stepwise increase in CSP regardless of posture. The upright tilt did not change operating AP (steady-state AP: 102 ± 4 mmHg in supine posture, 102 ± 5 mmHg in upright tilt posture). The upright tilt increased operating renal (100 a.u in supine posture, 148 ± 19 a.u. in upright posture) and cardiac SNAs (100 a.u in supine posture, 155 ± 21 a.u. in upright posture) by similar magnitudes.

Figure 9 showed the discharge characteristics of the renal and cardiac SNAs obtained from the same animal studied in Fig. 1. These SNAs were similar to some extent regardless of baroreflex condition and posture. In the supine posture (Fig. 9*A*), first, these SNAs were weakly pulse synchronous and had slower fluctuations with a time cycle of ~1.7 s in the baroreflex closed-loop condition, where CSP was artificially matched with systemic AP. The CSP and AP also had fluctuations with the same time cycle. Second, in the baroreflex open-loop condition, where CSP was fixed at 40 mmHg (the CSP level was chosen because it maximized these SNAs) without pulse, these SNAs had neither a pulse rhythmicity nor the slower fluctuation observed in the closed-loop condition. These discharge characteristics of SNAs were also observed in the 60° upright posture (Fig. 9*B*), although the amplitude of SNAs were larger at upright tilt than supine posture.

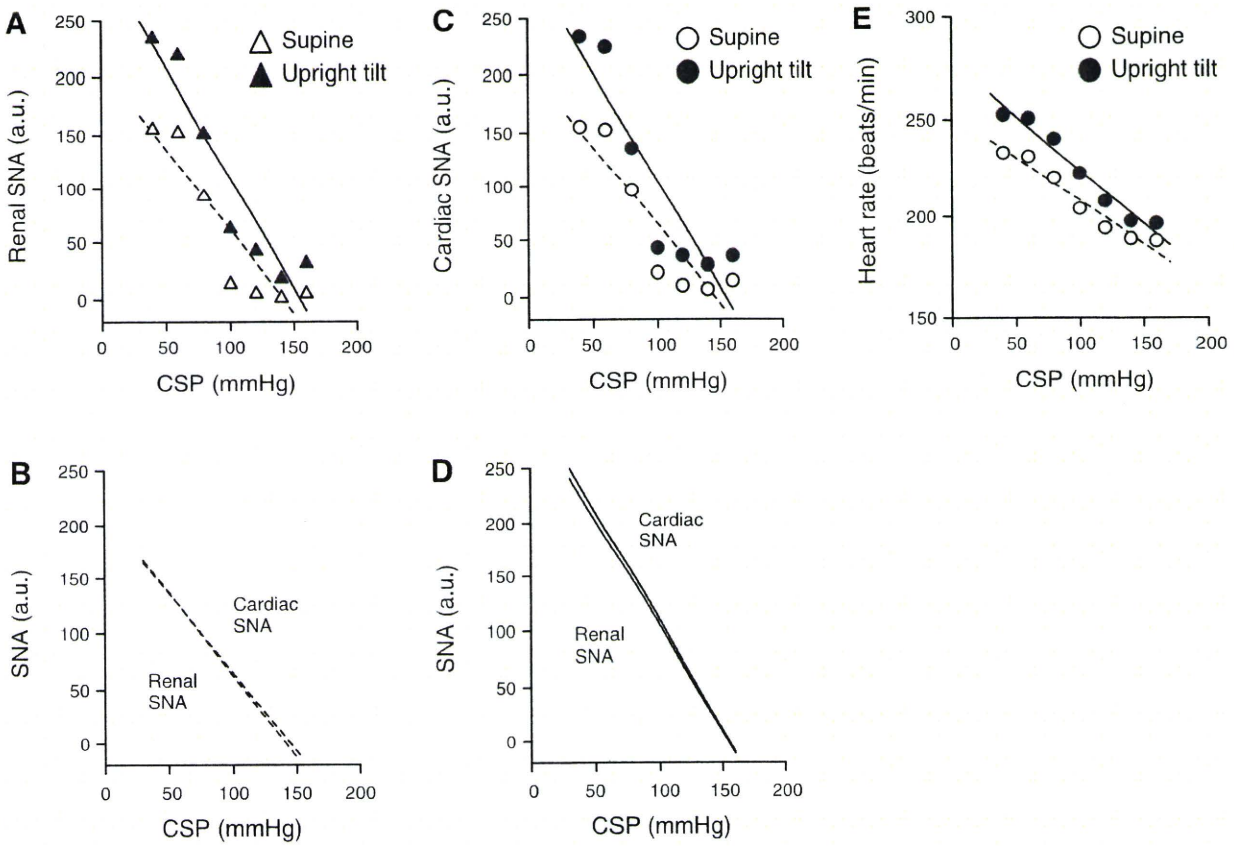

Fig. 4. Example of a model of the data shown in Fig. 2 using a simple regression line. Dotted and solid lines show the data in the supine and 60° upright tilt postures, respectively. The upright tilt shifted the baroreflex lines to a higher SNA similarly in renal (*A*) and cardiac SNAs (*C*). The lines were superimposed between these SNAs in the supine (*B*) and upright tilt postures (*D*). The upright tilt also shifted the baroreflex line of HR upward (*E*).

Baroreflex control of HR. In the representative time-series data, HR decreased in response to a stepwise increase in CSP in the 0° supine posture (Fig. 1*A*) and during 60° upright tilt (Fig. 1*B*). The upright tilt shifted the CSP-HR relationship upward to a higher HR (Fig. 2*E*), although HR was averaged for the last 10 s of each CSP level to investigate the steady-state, not transient, response to stepwise change in CSP.

Averaged data from all animals showed that the upright tilt shifted the CSP-HR relationship upward to a higher HR (Fig. 5*E*). When the static relationship between CSP and HR was fitted to a nonlinear reverse-sigmoidal curve (Fig. 6*E*), the P_1 (the range of HR response to CSP) and the maximal gain (at the midpoint of the logistic function) were larger at upright tilt than in the supine posture (Table 2), whereas P_2 (the coefficient of gain), P_3 (the midpoint CSP of the logistic function), and P_4 (the minimum value of HR) were not different between postures (Table 2). When the static relationship between CSP and HR was fitted to a linear regression line (Fig. 8*E*), the upright tilt increased the slope of regression from 0.46 ± 0.3 to 0.60 ± 0.3 beats·min^{-1}·mmHg^{-1}. The upright tilt increased operating HR (steady-state HR; 204 ± 11 beats/min in supine posture, 220 ± 12 beats/min in upright tilt posture).

DISCUSSION

Arterial baroreflex control of SNA is considered to have an important role to maintain AP under orthostatic stress against gravitational fluid shift directed toward the lower part of the body (15). In addition, we (8) recently reported that upright tilt resets arterial baroreflex control of renal SNA to increase orthostatic sympathetic activation. However, it remains unknown whether upright tilt resets arterial baroreflex control of SNA innervating to cardiovascular organs (i.e., the heart) other than the kidney. One major new finding in this study is that 60° upright tilt resets arterial baroreflex control of SNA to higher SNA similarly in renal and cardiac SNAs. This supports our hypothesis that upright tilt causes a parallel resetting of arterial baroreflex control of renal and cardiac SNAs in anesthetized rabbits.

Some regional differences between renal and cardiac SNAs certainly have been reported under some physiological conditions. First, for example, the dynamic high-pass characteristics in baroreflex control of SNA were greater in cardiac SNA than renal SNA (6, 10). Second, activating left atrial receptors increased cardiac SNA but decreased renal SNA (9). Last, hypoxia reset the AP-SNA relationship to higher AP and SNA in renal SNA but to lower AP and SNA in cardiac SNA (4). These lines of evidence indicate that renal and cardiac SNAs respond differently to specific physiological stimulation and stress (14).

However, our results indicate that upright posture induces a parallel resetting in arterial baroreflex control of renal and cardiac SNAs in the static characteristics. In agreement with previous studies (6, 7), the CSP-renal SNA reverse-sigmoidal curve was superimposable to the CSP-cardiac SNA curve in

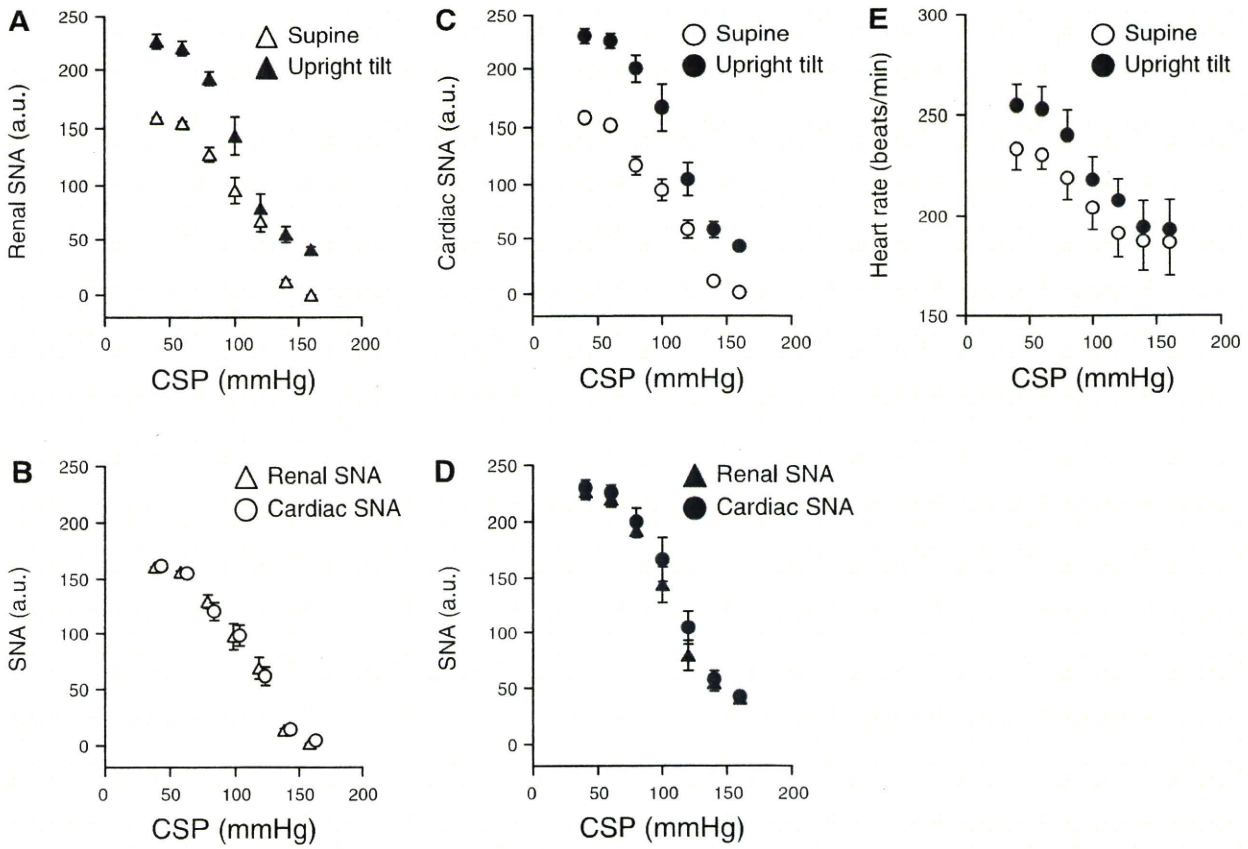

Fig. 5. Averaged data of arterial baroreflex control of renal (*A*) and cardiac SNAs (*C*) and HR (*E*) from all animals (n = 8). Open and filled symbols show the data in the supine and 60° upright tilt postures, respectively. The upright tilt shifted the baroreflex control of SNA to a higher SNA similarly in the CSP-renal SNA (*A*) and CSP-cardiac SNA relationships (*C*). *B* and *D* represent the superimposing of baroreflex control of SNA between renal and cardiac SNAs in both the supine and upright tilt postures, respectively. The upright tilt also shifted the baroreflex control of HR upward (*E*). Data are means ± SD.

the supine posture. This indicates that static nonlinear characteristics in arterial baroreflex control of renal SNA matched those of cardiac SNA in the posture. In addition, since upright tilt posture shifted the CSP-SNA curves upward similarly in renal and cardiac SNAs, the static nonlinear characteristics in arterial baroreflex control of renal SNA also matched those of cardiac SNA in upright tilt posture. These results were consistent with the close correlation between renal and cardiac SNAs during forced CSP changes with supine and upright tilt postures. They might also be consistent with a numerical simulation study indicating parallel responses of renal and cardiac SNAs to physiological pressure perturbations (AP change) (6).

Our results indicate that upright posture resets arterial baroreflex control of HR to a higher HR. This is consistent with the results of baroreflex resetting for cardiac SNA under upright tilt, because the P_1 (the response range) and the maximal gain (at the midpoint of the logistic function) were larger in both CSP-HR and CSP-cardiac SNA relationships. The parallelism suggests that cardiac sympathetic efferent was a dominant determinant for HR in the present experimental condition with cutting of vagal nerves. Our results could be consistent with the increase in the baroreflex gain for HR assessed by a neck pressure/suction device in humans (11).

Limitations. The present study has several limitations. First, we excluded the efferent effect of vagally mediated arterial baroreflex and an anesthetic agent that could affect baroreflex control of SNA. Second, the vascular isolation of carotid sinus might decrease brain blood flow under, in particular, upright tilt position. Third, we eliminated cardiopulmonary baroreflex by cutting bilateral vagal nerves. Earlier human studies have indicated that nonhypotensive hypovolemic perturbations do not change AP but reduce central venous, right heart, and pulmonary pressures and cause vasoconstriction. These observations have been interpreted as reflexes triggered by cardiopulmonary baroreceptors (5, 12). However, Taylor et al. (17) showed that small reductions of effective blood volume reduce aortic baroreceptive areas and trigger hemodynamic adjustments that are so efficient that alterations in AP escape detection by conventional means. In addition, Fu et al. (2) reported that arterial baroreceptors are consistently unloaded during low levels (i.e., −10 and −15 mmHg) of lower body negative pressure in humans. Accordingly, further studies are needed to understand the relative importance and mutual cooperation of arterial and cardiopulmonary baroreflexes in AP control during orthostatic stress. Fourth, we investigated arterial baroreflex during upright posture in rabbits, which are quadripeds. However, denervation of both carotid and aortic arterial baroreflexes caused postural hypotension of ~50 mmHg during 60° upright tilt in quadripeds [rabbits and rats (16)]. This suggests that even in quadripeds, arterial baroreflex has a very important role in maintenance of AP under orthostatic stress.

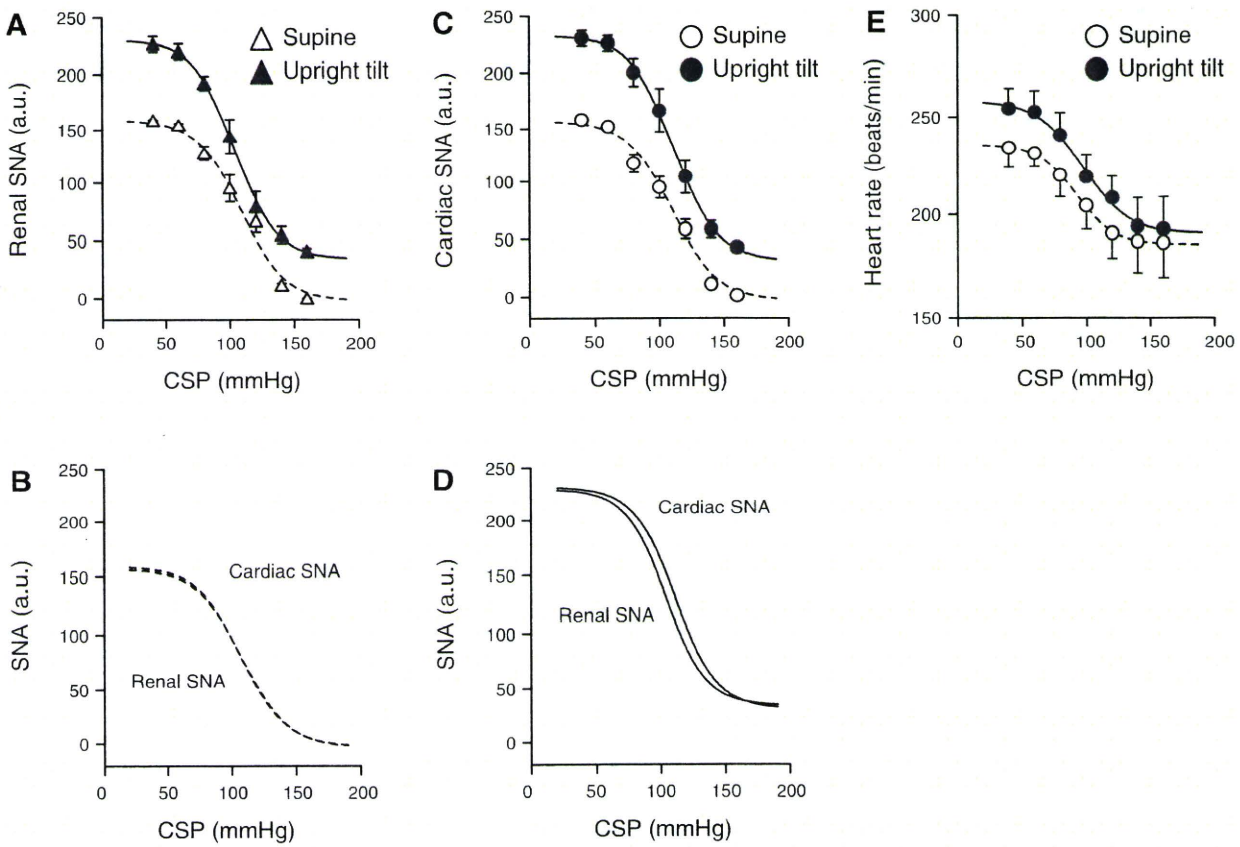

Fig. 6. A model of the averaged data shown in Fig. 5 using reverse-sigmoid 4-parameter logistic functions. Dotted and solid curves show the data in the supine and 60° upright tilt postures, respectively. The upright tilt shifted the baroreflex curves to a higher SNA similarly in renal (*A*) and cardiac SNAs (*C*). The curves were superimposed between these SNAs in the supine (*B*) and upright tilt postures (*D*). The upright tilt also shifted the baroreflex curve of HR upward (*E*).

Last, although we used two widely used traditional models to analyze the relationship between CSP and SNA, both have limited abilities to reproduce actual data. The nonlinear reverse-sigmoidal curve parameterized by a four-parameter logistic equation model provided high r^2 values (0.92–0.97) regardless of SNA type and posture. However, we failed to observe a saturation of SNA at the lowest CSP level in some cases (40 mmHg; Fig. 3, *A* and *B*, in upright tilt position). Lots of earlier studies have applied the model to AP and SNA (or HR) data under pharmacological perturbation (i.e., nitroprusside, phenylephrine) (1, 14), although it is difficult to observe clear saturation and/or threshold in the data. In contrary, the simple linear regression line model provided lower r^2 values (0.80–0.89). The plotted data did not appear to lie on a simple line in individuals (Fig. 4). Accordingly, we cannot conclude whether the relation between CSP and SNA is sigmoid or not. This problem is not the purpose of this study. Importantly, without modeling, our data (Fig. 2 and 5) indicate the parallel resetting of arterial baroreflex control of renal and cardiac SNAs.

Table 1. *Effect of upright tilt on parameters of baroreflex control of renal and catdiac SNAs*

	Supine	Upright tilt
Renal SNA		
P_1, a.u.	161 ± 2	196 ± 5*
P_2, a.u./mmHg	0.08 ± 0.01	0.08 ± 0.02
P_3, mmHg	105 ± 6	104 ± 6
P_4, a.u.	2 ± 1	34 ± 6*
G_{max}, a.u./mmHg	−1.5 ± 0.4	−1.9 ± 0.4*
Cardiac SNA		
P_1, a.u.	160 ± 2	201 ± 5*
P_2, a.u./mmHg	0.08 ± 0.01	0.08 ± 0.02
P_3, mmHg	109 ± 6	111 ± 6
P_4, a.u.	2 ± 1	31 ± 6*
G_{max}, a.u./mmHg	−1.4 ± 0.4	−1.9 ± 0.4*

Values are means ± SD (n = 8) for the parameters of baroreflex control of renal and cardiac sympathetic nerve activities (SNAs). See *Eq. 1* in METHODS for definitions of the 4 parameters of the logistic function. *$P < 0.05$, supine vs. upright tilt.

In conclusion, upright posture causes a resetting in arterial baroreflex control of SNA in parallel in renal and cardiac SNAs in anesthetized rabbits.

GRANTS

This study was supported by a research project promoted by the Ministry of Health, Labour and Welfare in Japan (no. H18-nano-ippan-003, H21-nano-ippan-005), a Grant-in-Aid for Scientific Research promoted by the Ministry of Education, Culture, Sports, Science and Technology in Japan (no. 20390462), and the Industrial Technology Research Grant Program from the New Energy and Industrial Technology Development Organization (NEDO) of Japan.

DISCLOSURES

No conflicts of interest, financial or otherwise, are declared by the author(s).

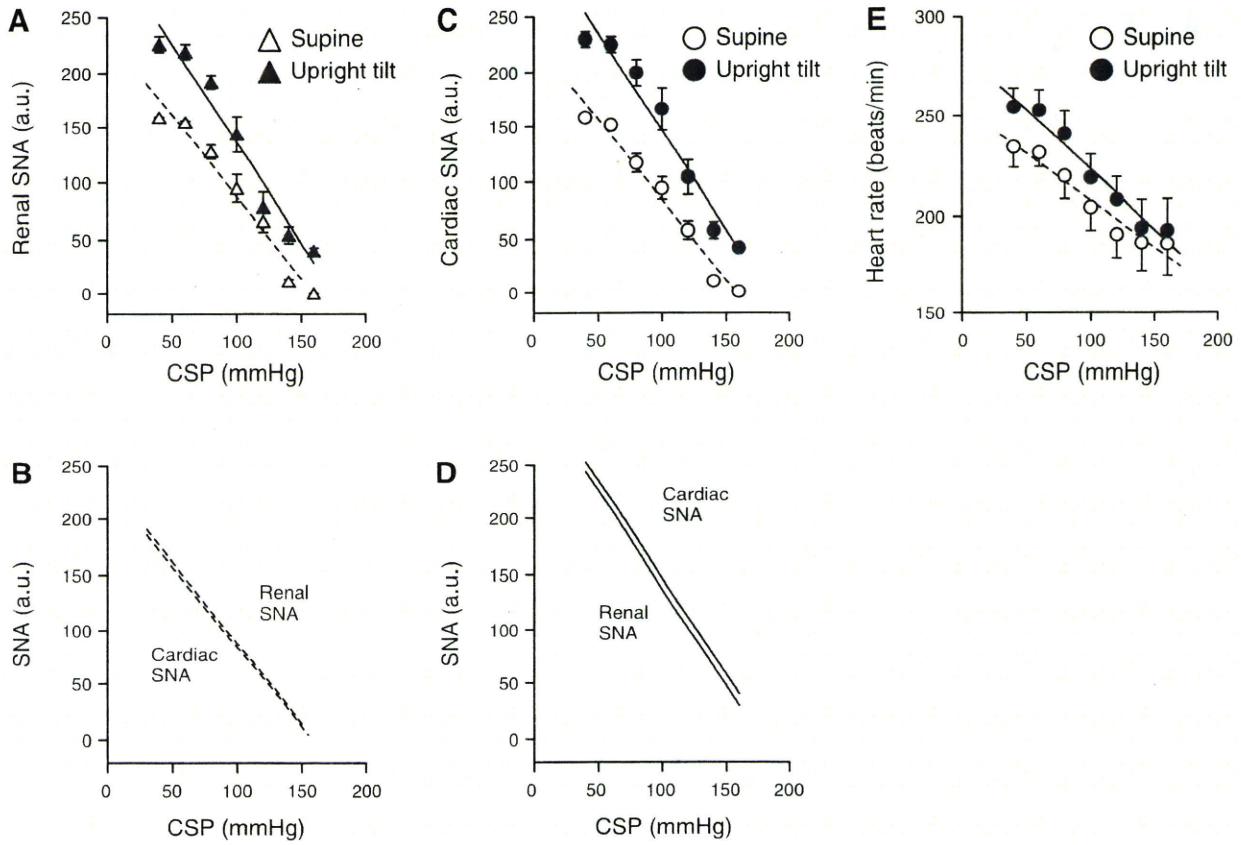

Fig. 7. A model of the averaged data shown in Fig. 5 using a simple regression line. Dotted and solid lines show the data in the supine and 60° upright tilt postures, respectively. The upright tilt shifted the baroreflex lines to a higher SNA similarly in renal (*A*) and cardiac SNAs (*C*). The lines were superimposed between these SNAs in the supine (*B*) and upright tilt postures (*D*). The upright tilt also shifted the baroreflex line of HR upward (*E*).

REFERENCES

1. **Eckberg DL, Sleight P.** *Human Baroreflexes in Health and Disease*. New York: Oxford Univ. Press, 1992, p. 3–299.
2. **Fu Q, Shibata S, Hastings JL, Prasad A, Palmer MD, Levine BD.** Evidence for unloading arterial baroreceptors during low levels of lower body negative pressure in humans. *Am J Physiol Heart Circ Physiol* 296: H480–H488, 2009.
3. **Glantz SA.** *Primer of Biostatistics* (4th ed.). New York: McGraw-Hill, 1997.
4. **Iriki M, Dorward P, Korner PI.** Baroreflex "resetting" by arterial hypoxia in the renal and cardiac sympathetic nerves of the rabbit. *Pflügers Arch* 370: 1–7, 1977.
5. **Johnson JM, Rowell LB, Niederberger M, Eisman MM.** Human splanchnic and forearm vasoconstrictor responses to reductions of right atrial and aortic pressures. *Circ Res* 34: 515–524, 1974.
6. **Kamiya A, Kawada T, Yamamoto K, Michikami D, Ariumi H, Miyamoto T, Shimizu S, Uemura K, Aiba T, Sunagawa K, Sugimachi M.** Dynamic and static baroreflex control of muscle sympathetic nerve activity (SNA) parallels that of renal and cardiac SNA during physiological change in pressure. *Am J Physiol Heart Circ Physiol* 289: H2641–H2648, 2005.
7. **Kamiya A, Kawada T, Yamamoto K, Michikami D, Ariumi H, Miyamoto T, Uemura K, Sugimachi M, Sunagawa K.** Muscle sympathetic nerve activity averaged over 1 min parallels renal and cardiac sympathetic nerve activity in response to a forced baroreceptor pressure change. *Circulation* 112: 384–386, 2005.
8. **Kamiya A, Kawada T, Yamamoto K, Michikami D, Ariumi H, Uemura K, Zheng C, Shimizu S, Aiba T, Miyamoto T, Sugimachi M, Sunagawa K.** Resetting of the arterial baroreflex increases orthostatic sympathetic activation and prevents postural hypotension in rabbits. *J Physiol* 566: 237–246, 2005.
9. **Karim F, Kidd C, Malpus CM, Penna PE.** The effects of stimulation of the left atrial receptors on sympathetic efferent nerve activity. *J Physiol* 227: 243–260, 1972.
10. **Kawada T, Shishido T, Inagaki M, Tatewaki T, Zheng C, Yanagiya Y, Sugimachi M, Sunagawa K.** Differential dynamic baroreflex regulation of cardiac and renal sympathetic nerve activities. *Am J Physiol Heart Circ Physiol* 280: H1581–H1590, 2001.
11. **Ogoh S, Yoshiga CC, Secher NH, Raven PB.** Carotid-cardiac baroreflex function does not influence blood pressure regulation during head-up tilt in humans. *J Physiol Sci* 56: 227–233, 2006.
12. **Pawelczyk JA, Raven PB.** Reductions in central venous pressure improve carotid baroreflex responses in conscious men. *Am J Physiol Heart Circ Physiol* 257: H1389–H1395, 1989.
13. **Persson P, Kirchheim H.** *Baroreceptor Reflexes: Integrative Functions and Clinical Aspects*. Berlin: Springer, 1991.
14. **Ramchandra R, Hood SG, Denton DA, Woods RL, McKinley MJ, McAllen RM, May CN.** Basis for the preferential activation of cardiac sympathetic nerve activity in heart failure. *Proc Natl Acad Sci USA* 106: 924–928, 2009.
15. **Rowell LB.** *Human Cardiovascular Control*. New York: Oxford Univ. Press, 1993, p. 3–254.
16. **Sato T, Kawada T, Sugimachi M, Sunagawa K.** Bionic technology revitalizes native baroreflex function in rats with baroreflex failure. *Circulation* 106: 730–734, 2002.
17. **Taylor JA, Halliwill JR, Brown TE, Hayano J, Eckberg DL.** "Non-hypotensive" hypovolaemia reduces ascending aortic dimensions in humans. *J Physiol* 483: 289–298, 1995.